Photodynamic therapy-based combinations with immunotherapy in colon cancer treatment

Hao, Y.

04

Combinatorial Therapeutic Approaches with Nanomaterial-Based Photodynamic Cancer Therapy

This chapter was adapted from "Hao, Y., Chung, C. K., Yu, Z., Huis in 't Veld, R. V., Ossendorp, F. A., Ten Dijke, P., & Cruz, L. J. (2022). Pharmaceutics, 14(1), 120."

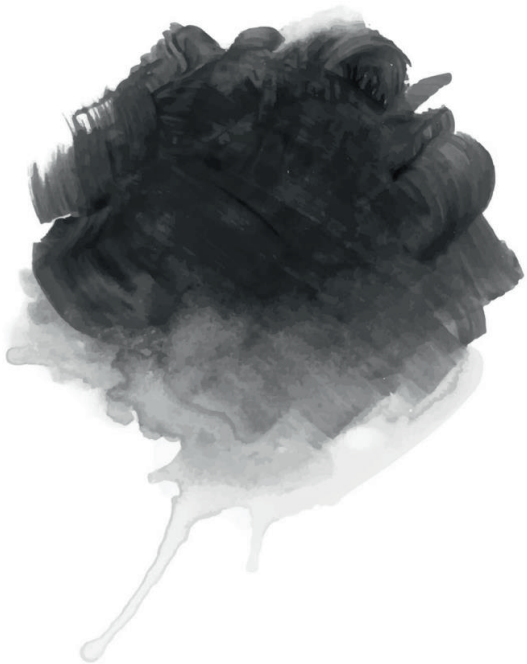

CHAPTER 4

Abstract

Photodynamic therapy (PDT), in which a light source is used in combination with a photosensitizer to induce local cell death, has shown great promise in therapeutically targeting primary tumors with negligible toxicity and minimal invasiveness. However, numerous studies have shown that noninvasive PDT alone is not sufficient to completely ablate tumors in deep tissues, due to its inherent shortcomings. Therefore, depending on the characteristics and type of tumor, PDT can be combined with surgery, radiotherapy, immunomodulators, chemotherapy, and/or targeted therapy, preferably in a patient-tailored manner. Nanoparticles are attractive delivery vehicles that can overcome the shortcomings of traditional photosensitizers, as well as enable the codelivery of multiple therapeutic drugs in a spatiotemporally controlled manner. Nanotechnology-based combination strategies have provided inspiration to improve the anticancer effects of PDT. Here, we briefly introduce the mechanism of PDT. Moreover, we discuss the current challenges facing the combination of PDT and multiple cancer treatment options, and we highlight the opportunities of nanoparticle-based PDT in cancer therapies.

Keywords: cancer photodynamic therapy; drug delivery; combined therapy; cancer vaccines; chemotherapy; radiotherapy; checkpoint inhibitor therapy

Introduction

Each year, about 10 million people die of cancer, accounting for about one-sixth of the worldwide mortality, thus causing a high societal and economic burden [1]. Patients in the early cancer stages (stage I/II) can often be efficiently treated by conventional approaches, such as surgery, chemotherapy, and radiation therapy [2]. However, more aggressive stages of cancer are difficult to treat; therefore, new therapeutic options are desired. In photodynamic therapy (PDT), a light source is used in combination with a photosensitizer and oxygen in order to induce cell death. PDT is used most commonly to treat acne and other medical conditions, including psoriasis and age-related macular degeneration [3]. Notably, its application to therapeutically target primary tumors with negligible toxicity and minimal invasiveness has gained great momentum. Patients are administered with a photosensitizer first, which accumulates in tumors. By exposure to

specific wavelengths of nonthermal light, the photosensitizer becomes activated from the ground to excited states, thereby providing energy for oxygen to generate reactive oxygen species (ROS), including hydrogen peroxide (H_2O_2), superoxide anions (O_2-), and hydroxyl radicals (OH−), and singlet oxygen ($^1O_2$) [4]. This destroys the organic constituents of the (tumor) cell structure, triggering apoptosis and necrosis of the cancer cells [5]. Furthermore, PDT can also achieve anti-tumor effects indirectly, by damaging the tumor vasculature and by activating immune responses [6].

Over the past 30 years, PDT has been tested clinically for different cancer types, especially superficial tumors, such as oropharyngeal cancer, esophageal cancer, and cutaneous carcinoma [7]. Due to the penetration limitations of traditional visible light into tissues, PDT has not been used for the treatment of large tumors that are growing in internal organs to date. The penetration constraints provide a challenge that needs to be overcome. Moreover, to enable PDT treatment of cancer relapses, further optimization and the development of treatment strategies utilizing PDT combined with currently available cancer treatment modalities are needed. Furthermore, a better understanding of the underlying mechanisms of such PDT combined therapies is required.

In this chapter, we introduce the most used co-delivery systems for combined therapies with PDT in cancer and summarize the recent Nanoparticle-Based PDT combination strategies, especially chemotherapy, and immunotherapy, among others, have been shown to be excellent combination partners of PDT. In light of the above, we provide a discussion on the potential and caveats of the NPs-based PDT combination in cancer treatment.

Nanomedicine-Based Combination Therapy Strategies for PDT

A few cancer types respond well to traditional methods such as surgery, radiotherapy, and PDT. Unfortunately, several solid tumors fail to respond due to therapy resistance, metastasis to distant organs, and induced recurrence problems in cancer patients [8]. Common mechanisms of metastasis include genomic instability, epigenetic modifications, epithelial-to-mesenchymal phenotype transition (EMT), remodeling the extracellular matrix, blood supply system, immune evasion microenvironment, and metastatic sites, among others [9–13]. Metastasis and therapy resistance may be addressed by the use of nanocarriers to improve the therapeutic index [14]. Employing specifically adapted nanoparticles for PDT-based combined therapy provides a promising platform for codelivery of multiple drugs (action in different modes) and PSs, with the advantages of minimizing potential toxicity in healthy tissues, improving drug efficacy, and excellent physicochemical properties [15]. Of note, a nanotechnology-based PDT combination displayed potential in preclinical studies by incorporating the features of diagnosis, therapy, and imaging. In this sense, highly encouraging results have been obtained through the combination of PDT with organic delivery systems (e.g., hydrogels, liposomes, and polymeric nanomaterials) and inorganic nanomaterials (e.g., metallic and silica NPs) (Figure 1).

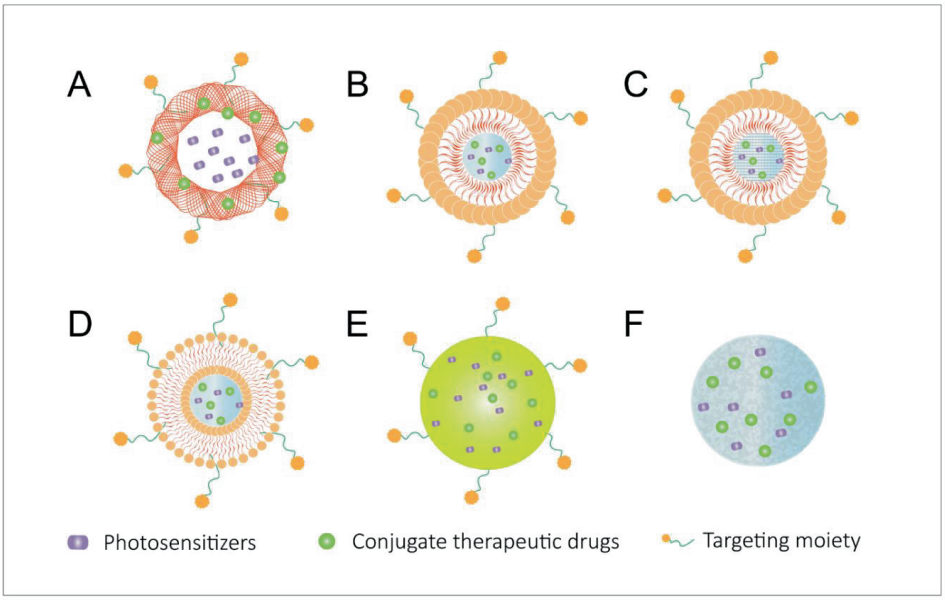

Figure 1. Most used codelivery systems for combined therapies with PDT in cancer, including (**A**) polymeric nanoparticles (PNPs), (**B**) nanostructured lipid carriers (NLCs), (**C**) solid lipid nanoparticles (SLNs), (**D**) liposomes, (**E**) gold nanoparticles (AuNPs), and (**F**) hydrogels.

The utilization of nanoparticles as delivery systems for PDT combinations can function in four different ways: (1) drug protection—protecting therapeutic cargos (e.g., drugs, antigens, and adjuvants) and PSs from degradation during blood circulation and prolonging their retention period; (2) tumor targeting—modifying the surface of the NPs with components that can interact with overexpressed molecules on tumor cell surface, thereby decreasing the nonspecific uptake of NPs to healthy cells and enhancing the accumulation of the NPs in tumors; (3) tumor normalization—overcoming PDT-enhanced hypoxia in the tumor microenvironment by intracellular oxygen supply by NPs or drug loading of hypoxia-activated prodrugs, such as tirapazamine (TPZ), apaziquone (EQ4), and banoxantrone (AQ4N), or overcoming the neutralization of PDT-generated ROS by high glutathione (GSH) in the tumor microenvironment through GSH-activated NPs or chemicals with the ability of intracellular GSH depletion; (4) medical imaging—protecting aggregation-caused quenching (ACQ) of PSs and providing opportunities to integrate multi-imaging modalities.

Nanoparticle-Based PDT Plus Surgery

PDT has been found to act as an effective adjuvant therapy in image-guided cancer surgery, especially in prostate cancer [16,17]. The PSs can improve the visualization of tumor margins and metastatic lymph node drainage, due to their fluorescent nature. Subsequent PDT treatment further ablates the remaining tumor tissues during surgical resection, thereby reducing tumor recurrence and significantly extending survival. Utilization of nanoparticles in PDT synergized with surgery to overcome ACQ of PSs during their introduction and increased the uptake and retention time of the PSs for

imaging guidance of the surgery [18]. For example, PS-loaded gold nanoparticles (AuNPs) [19], up-conversion nanoparticles (UCNPs) [20,21], and conjugated polymer (CP) nanoparticles [22] have shown promising potential to be used in imaging-guided surgery and PDT. A novel multimodal porphyrin lipoprotein-mimicking nanoparticle labeled with copper-64 (PLP) intrinsically integrates diagnosis (positron emission tomography (PET) imaging and fluorescence imaging) and PDT treatment in this platform [23].

Nanoparticle-Based PDT Plus Radiotherapy

Studies have demonstrated that nanoparticle-based PDT plus radiotherapy improved anti-tumor effects by improving the absorption efficiency and stability of agents (PSs and radio agents), thus reducing the side-effects of PDT and RT to healthy organs. For example, Wang et al. set up self-assembling nanoparticles (Ce6-R9-^{125}I-RGD-MNPs) of PS and radiotherapeutic peptides, which showed a better tumor-inhibitory effect compared to single therapy but with minimal toxic effects to normal tissues in Hela tumor-bearing mice [24]. A nanoparticle consisting of hafnium (radiosensitizer) and tetrakis (4-carboxyphenyl) porphyrin (TCPP, as PS) has been found to have a higher capacity to destroy tumor cells than single RT or PDT in a 4T1 murine breast cancer model because of longer tumor retention time [25]. This combination strategy has the potential to further improve the PDT efficiency in deep tumors due to the penetration ability of ionizing irradiation (X-ray) to the tumors. Liu et al. demonstrated that dibenzocyclooctyne (DBCO)-modified Hf-AIE coordination polymer nanoparticles (CPNs) has good biosafety, using hematoxylin and eosin (H&E) staining images of tumors. It can also greatly inhibit a 4T1 murine breast cancer model due to increased CPN tumor accumulation and prolonged retention time. Furthermore, CPNs have been found to have an improved anticancer effect against a deep tumor model (42.5% tumor growth suppression) [26].

In addition to the increased single-therapy threshold by the delivery system, PSs (e.g., Photofrin II and hematoporphyrin dimethyl ether; HPde) [27,28] and high-Z nanomaterials (e.g., gold nanoparticles (AuNPs), MoS_2/Bi_2S_3 nanosheets, and CuS nanoparticles) can act as specific radiosensitizers, in order to obtain an optimized anticancer effect. From this perspective, researchers have developed hyaluronic acid-modified Au nanocages (AuNPs-HA) integrating photoacoustic (PA) imaging, RT, and PDT at the same time. This multiple functional nanoplatform itself works as both radiosensitizer and PS, leading to better tumor growth suppression than each therapy alone in a 4T1 murine model. Additionally, the PA imaging-guided approach enabled more precise identification of the tumor location and size [29].

At a certain point, the improved absorption difference between healthy and tumor tissues by nanocarriers may minimize the resistance problem of RT. Geoffrey et al. generated MC540-SAO: Eu@mSiO_2 nanoparticles (MC540: a PS; SAO: Eu, a scintillator that converts X-ray photons to visible photons). These nanoparticles were used in combined PDT and RT. MC540-SAO: Eu@mSiO_2 NPs enhanced anti-tumor growth effects and reduced clonogenicity of RT-resistant cancer cells in an H1299 mouse model without detectable systematic toxicities [30]. Further studies have demonstrated that nanoparticle-based PDT-RT can have systemic synergistic anti-tumor effects through an enhanced

apoptosis rate by targeting different cellular components (e.g., cell membrane and DNA) leading to facilitated ROS diffusion, the release of damage-associated molecular patterns (DAMPs; molecules released from damaged or dying tumor cells can induce innate immune responses), and antigen expression [31]. These mechanisms have supported studies to explore the strategy of combining PDT-RT with immune checkpoint inhibitors in order to stimulate an activated immune system, especially $CD4^+$ and $CD8^+$ T cells. Immunotherapy PDT combinations are discussed in detail in Section 4.4. When combined with anti-PDL1, PDT-RT treatment results have shown tumor growth inhibition indices of primary and distant tumors as 99.5% and 98.0%, respectively, for CT26, and 94.7% and 92.2%, respectively, for SCC VII tumor models [32]. When further combined with an indoleamine 2,3-dioxygenase (IDO) inhibitor, which acts on tumor cells by enhancing antigen recognition, PDT-RT nanoparticles regressed both primary-treated tumors and distant untreated tumors by forming an *in situ* vaccine in a CT26 colon-rectal cancer murine model [33].

Nanoparticle-Based PDT Plus Chemotherapy

Chemotherapy (CT) is the main anti-tumor treatment modality, which works by inhibiting the process of cell growth and cell division by binding to tumor cell DNA. As shown in Figure 2, co-loading PSs and anti-tumor chemo drugs into the same delivery system can enhance the effects of single-therapy approaches. Some small-molecular inhibitors co-encapsulated with PSs can help PDT to greatly destroy primary tumors with lower recurrence or metastasis rates. Blocking angiogenic activity molecules or their receptors against tumors possibly upregulates expression of vascular endothelial growth (VEGF) and cyclooxygenase (COX)-2 during PDT [34,35]. Additionally, they can achieve a spatial cooperation anticancer effect via synergistic effects through enhancing immune responses by increasing immunogenic cell death (ICD) levels (ICD is defined by chronic exposure of DAMPs), type I interferon (IFN) secretion, and modulating immune cell subset activities [36]. Furthermore, the decreased effective dosage of therapeutic agents in a codelivery system can result in a reduction in side-effects while providing the potential of reducing multidrug resistance (MDR) [37]. Furthermore, some specific targeting ligands can be modified to the surface of NPs in order to enhance the tumor accumulation of drugs and decrease the severe side-effects of chemotherapy drugs due to their non-specificity, thus enhancing anti-tumor efficiency. For example, folic acid (FA), hyaluronic acid (HA), biotin, and antibodies have been utilized on the surface of dual drug-loaded nanosystems as active targeting ligands [38]. Yumin et al. conjugated RGD peptides to pH-sensitive polyethylene glycol (PEG) nanoparticles containing Ce6 as a PS and doxorubicin (DOX) for chemotherapy. These nanoparticles have a highly cytotoxic effect in vitro, due to improved cellular uptake. The NPs significantly enhanced the anti-tumor effect in an MDA-MB-231 tumor-bearing mouse model, with lower cardiotoxicity of DOX because of the superior tumor targeting and retention ability of NPs [39].

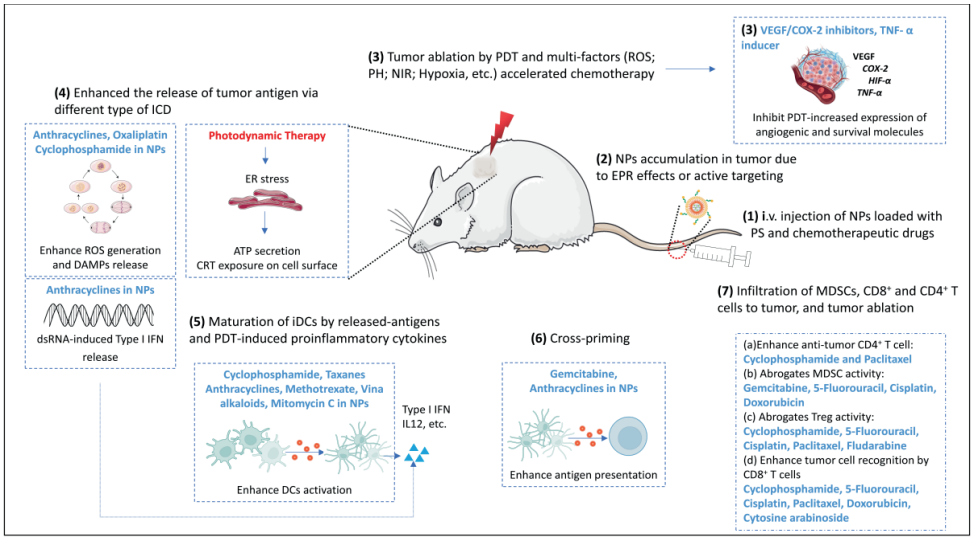

Figure 2. The mechanisms of NP-mediated chemo-photodynamic therapy enhance monotherapy indices and synergistically trigger robust antitumor immune responses for anti-primary and metastatic tumors: (1) intravenous injection of PSs and chemotherapeutic agents loaded with nanoparticles; (2) enhanced NP accumulation in tumor due to the tumor-targeting capability of NPs (EPR effects and targeting motif modification on NP surface); (3) primary tumor ablation by enhanced PDT and chemotherapy. PDT-caused vasculature rupture induced surviving tumor cells to produce more protumor factors in the tumor microenvironment. Antiangiogenetic mediators, such as VEGF and COX-2 inhibitors, help PDT to achieve more powerful tumor destruction and a lower recurrence or metastasis rate, by blocking tumor angiogenetic activity molecules or their receptors; (4) PDT and chemotherapy (anthracyclines, cyclophosphamide, and oxaliplatin) of the primary tumor to induce higher ICD levels and the release of tumor-associated antigens. Anthracyclines also induce dsRNA release from dead tumor cells, which can activate tumor-specific $CD8^+$ T cells by binding to Toll-like receptor-3 and inducing type I interferon production; (5) DC maturation and antigen presentation are enhanced by PDT-generated antigens, proinflammatory cytokines, and chemotherapeutic agents; (6) cross-priming in tumor lymph node; (7) Chemotherapeutic agents in NPs can improve PDT-induced immune responses by modulating the activity of immune cell subsets and by promoting tumor cell death.

Organic Nanoparticle-Based PDT Plus Chemotherapy

Organic NPs have attracted attention in the field of PDT plus chemotherapy (Table 1), due to their biosafety and biocompatibility profiles. Several well-developed structures have been widely used for PS and chemo-drug codelivery, including polymeric NPs, micelles, liposomes, hydrogels, and dendrimers.

Polymeric NPs used for PDT combination consist of naturally occurring (e.g., alginate, chitosan, and collagen) or synthetic polymer (e.g., polylactic acid (PLA), polyglycolic acid (PGA), or their copolymers, such as polyester (PLGA) and polyethylene glycol (PEG)), which can be hydrolyzed enzymatically into nontoxic byproducts in metabolic environments [40]. For example, highly tumorigenic cancer stem cells (CSCs) in tumors are one of the main reasons for chemotherapy resistance. Elisa et al. reported

the self-assembly of hyaluronic acid (HA)-coated polymeric nanoparticles using PEI-PLGA, docetaxel (DTX), and *meso*-tetraphenyl chlorine disulfonate (TPCS2a). After intravenous injection of NPs, HA@DTX/TPCS2a-NPs accumulated more in monolayers and mammosphere cultures enriched in CSCs ($CD44^{high}/CD^{24}$ low population) and elicited superior efficacy over monotherapies in reducing the self-renewal capacity. These nanomaterials showed great potential to overcome CSC-induced chemo-drug resistance and metastases [41].

Xue-Liang et al. designed and prepared macrophage cell membrane (CM)-coated liposomes to co-deliver nano-platinum (Pt) and verteporfin (VP). This lipid-based nano-Pt/VP@MLipo significantly inhibited tumor cell viability in 4T1 cells and a 3D 4T1 spheroid model. In vivo results showed that there was ~90% 4T1 tumor inhibition in the same period and extended mice survival (median survival 43 days), with no lung metastasis, compared to other treatments [42]. Another study reported hybrid PLGA/lipid-PEG NPs containing indocyanine green (ICG) and TPZ. Via NIR irradiation, ICG-based PDT directly kills the tumor by ROS generation, while consumption of oxygen during the PDT process can promote a degree of hypoxia at the tumor site(s), which may greatly activate the cytotoxicity of the hypoxia-activated TPZ through a cascade process. Furthermore, they demonstrated that this combination by PLGA/lipid-NPs had a synergistic inhibitory effect on primary tumor growth and metastasis-associated with enhanced the necrotic area (~95%) compared to the control group (~30%), via H&E analysis of tumor sections [43]. Micelles and hydrogels have also been studied as codelivery carriers to target tumor cells, due to their enhanced EPR effects. A thermal-responsive hydrogel based on a PCL-PTSUO-PEG copolymer designed by Zhongming et al. had the advantages of local targeting and sustained release. This in situ formed hydrogel encapsulated with DOX and ZnPC showed excellent cell-inhibitory effects in 5637 cells with a cell viability of 18.5% (4.8-fold that of free ZnPC-PDT), due to increased ROS generation. Enhanced ability of tumor control has been observed in a nude mice xenograft bearing 5637 cells [44]. Hua et al. found that self-assembled polyethyleneimine-nitroimidazole (PEI-NI) micelles provided a promising codelivery system for DOX and Ce6. This micelle-based combination of PDT and chemotherapy improved the therapeutic ratio of these modalities, by enhancing the stability and biocompatibility of agents, as well as dual trigger-induced highly cancer-selective drug release [45]. Taken together, organic nanoparticles provide effective delivery systems for PDT in combination with chemotherapy and are being currently studied in both preclinical tests and clinical trials.

Table 1. Preclinical studies on organic nanoparticles for codelivery in PDT plus chemotherapy.

PS	Chemo Drugs	Delivery System	Specific Function of Delivery System	Cancer Models	Therapeutic Outcomes of Combination	Ref
Polymeric Nanoparticles						

Ce6	DOX	RGD-PEG-DOX nanoparticles	pH-responsive; tumor targeting by RGD peptide	MDA-MB-231 cells, MCF-7 cells; MDA-MB-231 tumor-bearing mouse model	High cytotoxicity effect in vitro due to improved cellular uptake; significantly enhanced anti-tumor effect with lower cardiotoxicity of DOX, according to the pathological analysis	[39]
Ce6	Curcumin	Crosslinked polyphosphazene nanoparticles (FHCPCe NPs)	PH/redox dual-stimuli-responsive; dual-modal imaging (fluorescent imaging (FL) and computed tomography (CT))	HeLa xenograft cervical cancer mouse model	Synergistic anti-tumor activity both in vitro and in vivo	[46]
Ce6	DOX	MnO_2-loaded PCLA-PEG-PCLA NPs (CDM NPs)	Intratumoral self-sufficiency of O_2; trimodal imaging (FL, PA, MRI)	MCF-7 xenograft human breast tumors	Enhanced tumor growth inhibition and the inhibition ratio (IR) calculated by tumor weight was 92.35%, with no appreciable impact on body weight or the major organs in mice	[47]
HPPH	Camptothecin (CPT)	Polymeric nanoparticles	ROS-responsive; dual-imaging (PA and FL)	Nude mice bearing CT26 colorectal cancer	Effectively inhibit tumor proliferation and growth in vitro and in vivo	[48]
TPPS2a	DOX	Copolymer nanoparticles	O_2-evolving and ROS-activable; tumor targeting by F7 peptide	MCF-7/ADR tumor-bearing mice	Enhanced cell killing effects in vitro; prolonged survival time of combined therapy to 41 days, compared to NP-based PDT (32 days) and free DOX (25 days).	[49]
TPCS2a	DTX	Polymeric nanoparticles (HA@DTX/TPCS 2a-NPs)	Tumor targeting ability	$CD44^{high}$ MDA-MB-231 and the $CD44^{low}$ MCF-7 cells; mammosphere	Enhanced killing CSCs effects in vitro by 2D and 3D assay	[50]
TPCS2a	CPT	Double-layered polymeric nanoparticles	Tumor targeting due to HA	DTX-sensitive (HeLa-P, MDA-MB-231) and DTX-resistant (HeLa-R) cancer cells	Synergistic anti-tumor activity in vitro and reduced DTX dose in NPs by ~2.6- and 10.7-fold in HeLa-P and MDA-MB-231, respectively; reduced DTX doses in NPs by more than 100 times in DTX-resistant HeLa-R cells	[51]
Polymer PFV materials	Prodrug BDOX	DSPE-PEG-iRGD-PFV-BDOX conjugated polymer NPs	Tumor targeting by iRGD peptide; ROS-responsive	PC-3 human prostate cancer cells	Enhanced cancer cell killing effects in vitro due to enhanced tumor cell targeting and uptake	[52]
ICG	Oxaliplatin (OXP)	PLGA-PFP-OXP-ICG NPs	Photoacoustic and ultrasonic imaging	ID8 ovarian tumor mouse model	Improved anti-tumor effects on cancer cell due to enhanced DAMPs expression	[53]

IR780	DOX	Amphiphilic nanoparticles (F-IR780-PEG)	Intratumorally self-sufficiency of O_2; NIR-responsive; high oxygen capacity	Nude mice bearing MCF-7 human breast cancer	Remarkable therapeutic efficacy in killing tumor cells and destroying solid tumor	[54]
Hematoporphyrin (HP)	DOX	PEG-modified hematoporphyrin (HPP)-based NPs (HPPD)	Enhanced drug release at pH 5.8, along with laser radiation	MCF-7 human breast cancer cells and MHCC-97H human hepatoma cancer cells; nude mice bearing ADR/MCF-7 human breast tumors	A 12-fold decreased IC_{50} value due to improved drug penetration, resulting in promoted apoptosis in vitro; compared to free Dox, which failed to constrain tumor growth, combined therapy had efficient drug-resistant tumor ablation to an undetectable level in 2 weeks without inducing myocardial injury	[55]
Protoporphyrin (Por)	Epirubicin (EPI)	EPI-loaded cRGD-PEG-PH-PCL-Por	pH sensitivity; tumor targeting due to cRGD	CT26 murine colorectal tumor mouse model	Higher anticancer effectiveness, both in vitro with an IC_{50} = 0.47 μg/mL and in vivo, than that of free EPI	[56]
5,10,15,20-Tetraphenylchlorin (TPC)	PTX dimer (PTX2-TK)	RBC-membrane-coated (TPC-PTX2-TK-PEG) NPs	Prolonged blood circulation and improved tumor accumulation by coating RBC membrane	Nude mice bearing HeLa human cervical carcinoma	Enhances anticancer therapeutic activity; reduces systematic toxicity due to light-triggered drug release, as certificated by H&E staining and serum biochemical analysis of main organs	[57]
NPs	SN38	Multifunctional SN38-conjugated polymeric nanosystem (FA-PDA@PZM/SN38@BSA-MnO_2)	Intratumoral self-sufficiency of O_2; MRI imaging	Eca-109-esophageal tumor-bearing mice	Superior anti-tumor efficacy in Eca-109 tumor-bearing mice with low gastrointestinal toxicity and myelosuppression	[58]
Pyrolipid	Pt	Polymer-based core-shell nanoparticles	Drug release in a triggered manner	Human head and neck cancer SQ20B xenograft murine model	Superior potency and efficacy in tumor regression (83% reduction in tumor volume) at low drug doses in a cisplatin-resistant cancer model	[59]
ZnPc	DTX	Biodegradable core-shell nanoassemblies	Biodegradability and biosafety	HeLa cells, nude mice bearing A375 human amelanotic melanoma	Improved tumor growth-inhibitory effects compared to single therapy	[60]
Lipid-based NPs						

Photosan-2	Cisplatin (CDDP)	Lipid platinum-chloride nanoparticles (LPC NPs)	-	Nude mice bearing SAS squamous cell carcinoma	Significantly enhanced the therapeutic outcome in tumor volume reduction, compared to single therapies (~110.8% tumor growth inhibition); reduced the tumor growth rate	[61]
porphyrin	PTX	Porphyrin-lipid nanoemulsions	Imaging ability	KB xenografts tumor-bearing nude mice	Fourfold reduced PTX (1.8 mg/kg) dose in combined therapy with a superior anti-tumor effect, compared to single PTX therapy (7.2 mg/kg), resulting in reduced side-effects associated with chemotherapy	[62]
VP	Nano-Pt	Nano-Pt/VP@MLipo	Intratumoral self-sufficiency of O_2	4T1 breast tumor mouse model	Significantly inhibited tumor cell viability in vitro (2D and 3D model); enhanced tumor inhibition and extended mice survival time with no lung metastasis, compared to monotherapies	[42]
ICG	TPZ	Hybrid PLGA/lipid-PEG NPs	Tumor targeting by RGD peptide; improved penetration	3D tumor spheroids and orthotopic 4T1 breast tumor model	Synergistic cell-killing effect in vitro and effective primary tumor growth and metastasis inhibition; enhanced necrosis (~95% necrotic area) compared to control group (~30%), by analysis of the H&E tumor sections	[43]
Hydrogel						
ZnPc	DOX	Polymer hydrogel	Thermosensitive	Nude mice bearing 5637 human bladder tumors	Excellent cell-inhibitory effects in vitro, with cell viability of 18.5%, which is attributed to a high level of ROS generation (4.8-fold free ZnPC); slightly higher increased survival rate compared to chemo and PDT single groups	[44]
Micelles						
Mitoxantrone (MX)	MX	PEGylated UCNP (UPG) micelles	Tumor targeting by grafting with an anti-EpCAM antibody; dual-modality MR/UCL imaging	BEL-7404 liver carcinoma mouse model	94.4% cell death in vitro for combined therapy, compared to 67.6% for chemo only, which was attributed to the physicochemical property of micelles; remarkable anti-tumor effect with final tumor volume: 235.5 ± 87.4 mm^3, with negligible side-effects, as demonstrated by the images of H&E-stained major organs slices	[63]

IR780	DOX	Polydopamine nano clustered micelles (TPGS-IR780@PDA)	Enhanced intracellular accumulation by TPGS (a drug efflux inhibitor)	Nude mice bearing ADR/MCF-7 human breast tumors	Improved tumor-inhibitory efficiency, as evidenced by tumor sizes starting to reduce after 2 days of treatment (8 days for PDT group)	[64]
Ce6	DOX	Polymer-UCNP hybrid micelles (PUHMs)	NIR-triggered	HeLa human cervical carcinoma cells	High cytotoxicity for cancer cells in vitro, due to upconverted emission energy triggering ROS generation and faster DOX release	[65]
Ce6	DOX prodrug (PDOX)	Gd^{3+}-loaded copolymeric micelles conjugated with PS	Acid-switchable multimodal imaging (FL, PA, MR) capability	Nude mice bearing ADR/MCF-7 human breast tumors	Notably inhibited the tumor growth and completely eradicated two of the tumors, compared to single therapy; obvious DNA damage and membrane lysis revealed by H&E staining and notable apoptosis of tumor cells revealed by TUNEL staining	[65]
Ce6	DOX	Self-assembled polyethyleneimine-nitroimidazole (PEI-NI) micelles	Hypoxia trigger; PA imaging; tumor targeting by HA	LLC xenograft tumor-bearing mice	Significantly stronger anticancer efficacy than single therapy in vitro, evidenced by IC_{50} value of DOX (1.15 μg/mL) or Ce6 (0.16 μg/mL) in combined group lower than those of chemotherapy (>10 μg/mL) or PDT (0.75 μg/mL); compared therapy showed remarkably prolonged survival after 35 days observation.	[45]
5-(4-Carboxyphenyl)-10,15,20-triphenylporphyrin (Por)	GNA002	Micellar GNA002@cPRP	pH-sensitive; tumor targeting by cRGD; improved drug penetrability in vitro and prolonged tumor-retainability in vivo	HeLa, HN6, A375, MCF-7, and HN30 cancer cells and HeLa tumor-bearing mice	Decreased IC_{50} and increased cell apoptosis for combined group, compared to single therapy, due to increased ROS generation in vitro; tumor weight on day 14 was just 6.3% and 6.7% of that of the saline group of the HeLa and HN6 cancer-bearing mice, respectively, with negligible body weight loss; widespread cancer cell necrosis and apoptosis caused by combined therapy in H&E staining images; highest TUNEL expression and lowest cancer cell proliferation in the TUNEL-staining and Ki-67 staining images, respectively	[66]
Porphyrin	DOX	PEG-PGMA-PDPA Janus macromolecular brushes	Improved drug loading capability by π-π stacking; pH-responsive	4T1 breast cancer mouse model	In vitro studies showed the lowest cell viability (IC_{50}: 7.2 μg/mL TPP and 2.5 μg/mL DOX); in vivo studies confirmed that NP-based combination exhibited high phototoxicity and	[67]

					significant tumor inhibition efficacy	
Other Organic Nanoparticles						
Ce6	DTX	Redox-responsive polymer HA-cys-DHA/Ce6 (CHD)	Redox-responsive; Tumor-targeting by HA	MCF-7 breast tumor mouse model	Synergistic anti-tumor activity in vitro, due to inhibition of microtubule depolymerization, blocking cell cycle, and generating ROS, leading to best anti-tumor response in vivo	[68]
Ce6	Pt (IV)	Oxygen and Pt (II) self-generating conjugate	Intratumoral self-sufficiency of O_2	BALB/c mice bearing HeLa, HCT116, and MDA-MB-231 tumors	Enhanced anticancer efficacy both in vitro and in vivo; specifically, in vivo results showed that two of the five mice in combined treatment group were healed, and the tumor volumes of the other three mice decreased to very little	[69]
Ce6	TPZ	Self-assembly PA/HA-Ce6@TPZ NPs	Tumor targeting by HA; dual hypoxia-responsive	Nude mice bearing 4T1 breast cancer	Synergistic anticancer treatment due to PDT-mediated hypoxia-induced cascade TPZ therapy	[70]
Ce6	DOX	DOX-NPs/Ce6-microbubble complex	Local release due to the cavitation of NPs; enhanced extravasation and penetration due to energy of ultrasound	Nude mice bearing MIA-paca-2 human pancreatic carcinoma	Increased therapeutic effects in vitro by cell viability assay and in vivo by normalized tumor volume	[71]
Ce6	DOX	Hyperbranched polyphosphate SOHNPCe6/DOX	NIR-triggered	Nude mice bearing ADR/MCF-7 human breast tumors	Enhanced in vitro apoptosis inducing efficiency (56.82%) and lower cell viability at 72 h (80.46 ± 6.31%), compared to single-therapy group; high anti-tumor efficacy in drug-resistant breast cancer nude mouse model	[72]
Ce6	DOX	Ce6/Dox@NPs-cRGD	Tumor targeting by cRDG	MCF-7 xenograft human breast tumors	Significantly shrank tumor volume and prolonged survival time, compared to single therapies, with negligible body weight changes and staining organ slices	[73]
Ce6	DOX-precursor (CAD)	Co-assembly LA-CAT-CAD@Ce6 NPs	Tumor targeting by lactobionic acid; pH-sensitive; intratumorally	Nude mice bearing human MCF-7/ADR breast tumor cells	Enhanced cell killing and apoptosis efficiency in vitro and the most effective tumor inhibition and ablation ability	[74]

			self-sufficiency of O_2			
Ce6	Docetaxel (DTX)	Keratin nanoparticle	Monophasic release	DTX-sensitive HeLa (HeLa-P) and DTX-resistant HeLa (HeLa-R) cells	In monolayers, combined therapy had comparable cytotoxicity to free drugs toward HeLa-P cells, but synergic interaction in HeLa-R cells; induced stronger cytotoxicity and volume reduction rate in spheroids	[75]
Ce6	SN38	Carrier-free nanoparticles (SN38/Ce6 NPs)	Carrier-free	4T1 murine breast cancer cell lines	Significant increase in the inhibition rate by 85%, compared to single therapy, in vitro due to enhanced tumor accumulation and higher cellular internalization	[76]
PheoA	DOX	DOX-PheoA-alginate NPs)	NIR-triggered drug release	B16 tumor-bearing mice	Enhanced tumor growth inhibition by combined therapy with increased serum IFN levels	[77]
PheoA	DOX	Self-assembly PEG-thioketal-DOX NPs	ROS-responsive; phototriggered release	Nude mice bearing CT26 colorectal cancer	Enhanced anticancer therapeutic effect in vitro by cell viability assay and in vivo by tumor volume change, due to spatiotemporally controlled cascade drug release	[78]
VP	TMZ	Pluronic P85/F127 copolymers	Tumor targeting by biotin	T98-G, U87-MG, and U343 glioblastoma cells	Enhanced antiproliferative effect in vitro via different cell-cycle arrest mechanisms of drug action, especially at low TMZ concentrations and higher light doses	[79]
Hypocrellin B (HB)	PTX	Hyaluronic acid-ceramide nanoparticle	Tumor targeting due to HA	Nude mice bearing A549 human lung adenocarcinoma	Enhanced phototoxicity in vitro and improved anticancer efficacy, by tumor volume change, compared to single PDT and NP-based PDT	[80]
Pyropheophorbide a (PPa)	PTX	Self-assembly heterotypic chemo-photodynamic dimer	ROS-responsive	KB xenograft tumor-bearing nude mice, 4T1 xenograft tumor-bearing BABL/c mice	Synergistic anti-tumor activity, both in vitro and in vivo	[81]
Carbon dots (CDs)	Metformin (Met)	Traceable DOX/Met/BSA-HA-CDs	Dual-drug system; fluorescence imaging; tumor targeting by HA	MCF-7/ADR human breast cancer cells; S180 murine sarcoma tumor mouse model	Synergistic treatment achieved considerably highest cytotoxicity in vitro and enhanced cancer therapeutic efficiency in vivo, which was attributed to MET reducing the tumor O_2 consumption, resulting in increased the therapeutic	[82]

					efficiency of oxygen-consumed PDT	
??	DOX	Regenerated silk fibroin-based PC-Mn@Dox-NPs	Multimodality factors responding, resulting in controlled release; intratumoral self-sufficiency of O_2	4T1 breast cancer mouse model	Enhanced in vitro and in vivo anticancer efficacies, compared to all other combination approaches of PDT and DOX, due to multifactor triggered DOX release and oxygen-dependent PDT enhanced by self-sufficient O_2	[83]
ICG	Cisplatin (DDP)	Human serum albumin (HSA)-ICG-DDP NPs	NIR-triggered drug release	HSC human oral squamous cell cancer cells and NCM-460 colonic epithelial cells	Improved cytotoxicity for cancer cells in vitro due to higher ROS generation; significantly enhanced tumor growth inhibition compared to 632.06 ± 52.49 mm^3 in the NP-PDT group and 482.25 ± 42.69 mm^3 in the NP-chemotherapy group	[84]
ZnPC	DOX	Phthalocyanine-conjugated Glyco-NPs	pH-responsive; good colloidal stability; tumor targeting owing to GLUT5	3T3, MCF7, and MDA-MB-231 human breast cancer cells	High cytotoxicity effect in vitro, due to higher cellular internalization and induction of ROS generation	[85]
ICG	Bromoisophosphoramide mustard intermediate (IPM-Br)	Semiconducting polymer NPs	Light-responsive; intratumoral self-sufficiency of O_2; NIR imaging	Nude mice bearing 4T1 breast cancer cells	Synergetic anticancer effects due to improved chemo prodrug efficiency (4.3-fold higher, compared with its prodrug-free counterpart) due to PDT-enhanced degree of hypoxia; increased photodynamic efficacy (18-fold higher than ICG)	[86]
Boron-dipyrromethene (BODIPY)	Lenvatinib (VEGFR-inhibitor)	Self-assembling NPs (LBPNPs)	PH-sensitive	Human HCC cell lines Hep3B and Huh7	Effectively inhibited tumor growth in vitro by promoting the cascade of caspase apoptotic protease	[87]

Inorganic Nanoparticles-Based PDT Plus Chemotherapy

Inorganic NP-based PDT-chemotherapy combinations have enhanced therapeutic efficiency, due to their high stability, lower degradation rate, and ease of surface modification (Table 2). For example, one group developed a gold-caged organic/inorganic integrating nanoparticle (PTX-PP@Au NPs) encapsulating paclitaxel (PTX). In this multifunctional platform, AuNPs blocked the TRPV6 ion channel in androgen-resistant prostate cancer when under irradiation by NIR (808 nm) laser, and facilitated PTX release obtained an enhanced chemotherapeutic efficiency, both in vitro and in vivo [88].

In addition to gold nanomaterials, up-conversion NPs (UCNPs) have many attractive properties in PDT combined applications, through the conversion of NIR light into UV/Vis's wavelengths with high penetration into tumor tissues and lower phototoxicity. Lanthanide ion-doped mesoporous hollow cerium oxide UCNPs loaded with DOX (Ce-UCNPs) were synthesized by Yao et al. for NIR-triggered PDT and chemotherapy treatment of malignant glioma cancer. This nanocarrier is pH-sensitive and intracellular endogenous H_2O_2-responsive, resulting in the strong synergistic anti-tumor efficacy of combined therapy due to accelerated DOX release and self-sufficient O_2. Remarkable tumor cell viability inhibition has been observed in vitro; 28.2% of tumor cells survived after NP-based combined treatment, compared to 56.1% with DOX-loaded Ce-UCNP without irradiation. In a U87MG malignant glioma cancer mouse model, enhanced tumor growth inhibition and increased apoptosis/necrosis of tumor cells with negligible systemic toxicity were observed [89].

Ceramic NPs are another widely explored delivery vehicle for chemo-PDT; inorganic nanoparticles are often used due to their high biocompatibility and stability. Commonly used inorganic NPs in chemo-PDT include silica (SiO_2) NPs, titanium oxide (TiO_2) NPs, and calcium carbonate ($CaCO_3$) NPs. DOX-loaded mesoporous TiO_2 NPs (MTN/DOX) were produced, after which dual targeting components were grafted onto the surface (HA and ADH-1, a cyclic pentapeptide) to synthesize the final formulation This ADH-1-HA-MTN/DOX NP can be photoexcited with UV having a wavelength from 320 to 400 nm. Under X-ray irradiation, TiO_2 NPs produced ROS to directly kill tumor cells; these effects were further enhanced with higher accumulation of the dual-targeting nanosystem in $CD44^{high}$ tumor cells and EMT process blockage [90]. Furthermore, the shortcomings of X-ray-induced TiO_2 activation as PDT, including nonspecific harmful effects to normal cells and weak penetration in deep tumor tissues, can be circumvented by loading another PS into the core of the NP. For example, Zhang et al. reported ROS-responsive ZnPC-sensitized TiO_2 NPs conjugated with chlorambucil (CBL) ($mTiO_2$-BCBL@ZnPC NPs). This system, when triggered by NIR, has several advantages, including higher penetration, effective therapeutic effects, biosafety, and low side-effects. Moreover, PDT-generated ROS (H_2O_2) will cleave the phenylboronic ester between CBL and the NP, inducing CBL release activation and enabling a spatial and temporal light-triggered combination therapy [91].

SiO_2 NPs are popularly used for PDT combinations because they are easily surface-functionalized, by adjusting their pore sizes. However, the drawback of silica NPs is that they are sometimes recognized and cleared by the mononuclear phagocyte system (MPS). Thus, several studies have focused on mesoporous SiO_2 NPs (MSNs) coated with PEG or a membrane layer of erythrocytes, white blood cells, cancer cells, and/or bacteria to improve the application efficiency in cancer therapy [92]. For example, one group generated leukocyte/platelet hybrid membrane-camouflaged dendritic large pore MSNs (LPHM@DDI NPs), loaded with the NIR fluorescent dye IR780 and DOX as a model drug for chemotherapy. The hybrid membrane coating assisted the MSNs to escape from biological clearance, thus extending their circulation time. The tumor-targeting ability was further improved by the LFA-1/ICAM-1 interaction-dependent tumor vascular targeting and crossing effects. As a result, synergistic cytotoxicity and apoptosis-inducing

activity were achieved in vitro. Moreover, effective tumor growth suppression and recurrence prevention were achieved in TNBC mice, through the inhibition of cancer cell proliferation and mitigation of angiogenesis [93].

Table 2. Preclinical studies on inorganic nanoparticles for codelivery in PDT plus chemotherapy.

PS	Chemo Drugs	Delivery System	Specific Function of Delivery System	Cancer Models	Therapeutic Outcomes of Combination	Ref
Gold NPs						
Au NPs	PTX	PTX-loaded pluronic-PEI@Au NPs	NIR-sensitive; ion channel inhibition	Nude mice bearing PC3 human prostate cancer	Enhanced therapeutic efficiency in vitro and in vivo, with low toxicity on liver function and minimal side-effects to normal organs	[88]
Up-conversion NPs						
CeO_2 NPs	DOX	Lanthanide ion-doped mesoporous hollow cerium oxide UCNPs (Ce-UCNPs)	pH-sensitive; intratumoral self-sufficiency of O_2 due to H_2O_2-responsive ability	U87MG malignant glioma tumor mouse model	Remarkable cell viability inhibition in vitro and tumor growth inhibition, compared to treatment with DOX or PDT, with negligible systemic toxicity (little body weight difference between groups)	[89]
$ZnFe_2O_4$	Pt (IV) prodrugs	UCNPs-Pt (IV)-$ZnFe_2O_4$, denoted as UCPZ	Multimodality bioimaging (UCL, CT, MRI, and PA); inhibited biological clearance; enhanced tumor accumulation	U14 cervical tumor mouse model	Significantly enhanced anti-tumor effect in vivo	[94]
$ZnFe_2O_4$	DOX	UCNPs with a mesoporous $ZnFe_2O_4$ shell (UCNPs@mSiO$_2$)	Trimodal imaging (CT, UCL, MRI)	HeLa xenograft cervical tumor mouse model	High anticancer effectiveness both in vitro and in vivo	[95]
Rose Bengal (RB)	DOX	UCN@mSiO$_2$-(Azo + RB) nanoimpellers	Faster drug release due to Azo molecules	HeLa human cervical carcinoma cells	High cytotoxicity effect for cancer cells in vitro	[96]
Rose Bengal (RB)	Pt (IV) prodrugs	Biocompatible core-shell-shell UCNPs (PEG/RB-Pt (IV)-UCNPs)	NIR-triggered drug release	A2780 and A2780cisR human ovarian cancer cells	Improved cytotoxicity for both cisplatin-sensitive and -resistant human ovarian cancer cells in vitro	[97]
Rose Bengal (RB)	DOX	Cancer cell membrane	ROS-sensitive; inhibited biological clearance;	Primary 4T1 murine model; Metastatic Luc-4T1 breast	Enhanced uptake in tumor cells and deeper penetration in spheroids; strong synergistic anti-tumor	[98]

		(CM)-cloaked UCNPs	enhanced tumor accumulation	orthotropic tumor model	efficacy and synchronously causes increased DAMPs release, leading to tumor-specific immunity; when combined with anti-CD73 antibodies, had a better effect on lengthening the period of survival and inhibiting lung metastasis than monotherapies associated with stronger systemic cytotoxic T-cell responses	
Rose Bengal (RB)	DOX	NIR-triggered ROS-sensitive (UCN/SiO_2-RB + DOX) @PPADT NPs	NIR-triggered drug release	HeLa human cervical carcinoma cells	Achieved a better inhibitory effect on cancer cell in vitro at concentrations over 100 mg/L than single therapy	[99]
RBHA	Pt	CaF2: Yb^{3+}/Er^{3+} UCNPs coated with NaGdF4 shells (UCNPs-RBHA-Pt-PEG)	Multimodality bioimaging (UCL, MRI)	CT26 murine colorectal carcinoma cells	Visibly decreased tumor sizes for combined therapy group at a low irradiation power density (0.35 W/cm^2, 6 min)	[100]
Methylene blue (MB)	DOX	NaYF4: Yb,Er UCNPs	Tumor targeting due to anti-HER2 peptide	SKBR-3 (HER2-positive) and MCF-7 (HER2-negative) breast cancer cells	Significant decline in the cell viability by 95%, compared to 77% for chemo-drug and 84% for PDT only in vitro; cell viability was suppressed by 66% in a 3D model of SKBR-3 tumor spheroids, due to improved uptake of NPs	[101]
ZnPc	DOX	Protein-polymer bioconjugate-coated multifunctional UCNPs	Excellent water solubility, good stability, and low toxicity; real-time imaging capability	HeLa human cervical carcinoma cells	Enhanced tumor cell killing efficiency in vitro	[102]
Ce6/ZnPc /methylene blue (MB)	DOX	Red-emitting up-converting nanoparticles (α-CD-UCNPs)	-	A549 human epithelial lung cancer cells	Higher therapeutic efficacy, relative to the individual means, for cancer therapy in vitro	[103]
Polyelectrolyte brushes (PFNS)	AQ4N	pH-sensitive Mn-$Ca_3(PO_4)_2$ (MnCaP) layer-coated UCNP@PFN	pH-sensitive; hypoxia-activated; multi-imaging (MRI, FL, UCL)	HeLa human cervical carcinoma cells	Enhanced therapeutic effect, thereby reaching a tumor inhibition rate as high as 83%; highest level of cell apoptosis, as evidenced by H&E staining of tumor slices	[104]
Graphene oxide (GO)	DOX	UCNPs-DPA-NGO-PEI-DOX	UCL imaging; improved drug	U14 murine liver cancer xenograft	Substantially superior cell killing effects in vitro, due to sensitive disulfide bond;	[105]

			loading capability	tumor mouse model	higher tumor inhibition efficiency than monotherapies	
UCNPs	DOX	Core/shell structure SPTP@UCNP-RB NPs	NIR-controlled; tumor targeting to E-selectin; intratumoral self-sufficiency of O_2	Multicellular spheroid model; 4T1 murine breast cancer model	Synergistic anticancer effects and improved ICD levels in cells; enhanced uptake, penetration, and anti-tumor efficacy against multicellular spheroids; synergistically destroyed the orthotopic tumors and efficiently suppressed lung metastasis by cascade-amplifying systemic anti-tumor immunity through induction of ICD with $CD8^+$/$CD4^+$ T-cell infiltration and IL-6/IL-10 secretion	[106]
Ceramic Nanoparticles (Silicon dioxide Nanoparticles)						
Ce6	Pt (IV) prodrugs	MSNs/Ce6/Pt	Biocompatibility and stability; higher cellular uptake	Cisplatin-resistant A549R lung cancer cells	Improved treatment efficiency due to elevated cellular ROS level in vitro	[107]
Ce6	DOX	Erythrocyte-mimetic MSNs (RMSNs-Dox/Ce6)	Biocompatibility and stability; high loading capacities; irradiation sensitive; inhibited biological clearance; enhanced tumor accumulation	4T1 breast tumor mouse model	Effective cell killing ability, up to 92.1% cell death after treatment, compared to 75.2% in the NP-based chemotherapy group; enhanced tumor inhibition rate (91.4%), which was significantly higher than PDT single (68.9%) and chemotherapy single (73.7%) therapy, respectively; inhibited 75.1% metastatic foci to lung, which was more effective than monotherapies	[108]
TMPyP	DOX	MSN@SiNPs@ TMPyP-FA	Biocompatibility and stability; biological autofluorescence; tumor targeting by HA	MCF-7 human breast carcinoma cells and A549 human lung cancer cells	High cytotoxicity for tumor cells in vitro	[109]
IR780	DOX	Leukocyte/platelet hybrid membrane-camouflaged dendritic large pore MSNs	Biocompatibility and stability; tumor targeting by P-selectin/CD44 binding; inhibited biological	4T1 breast tumor mouse model	Synergistic cytotoxicity and apoptosis-inducing activity in vitro; effective tumor suppression and recurrence prevention in vivo through directly killing tumor cells	[93]

		(LPHM@DDI NPs)	clearance; enhanced tumor accumulation		and indirect anti-angiogenesis	
ICG	TPZ	Erythrocyte and tumor cell membrane camouflaged MSNs (IT@MSN@RTM)	Biocompatibility and stability; inhibited biological clearance; enhanced tumor accumulation; irradiation sensitive	4T1 breast tumor mouse model	1.3 times tumor inhibition rate of combined therapy, compared to 47% in the PDT treatment group alone	[110]
HCE6	OXP	OH-MSNs	Biocompatibility and stability; pH-sensitive	Nude mice bearing FRH0201 human hilar cholangiocarcinoma	Enhanced proliferation-inhibitory effects and killing effect of oxaliplatin in NPs in vitro; much more effective in inhibiting tumor growth in vivo compared with O-MSNs	[111]
Telluriu m (Te)	PTX	Double hydroxide gated MSNs (MT@L-PTX@FA)	Biocompatibility and stability; sustained release; pH-sensitive; tumor targeting by FA	HepG2 human hepatocyte carcinoma cells	Enhanced cancer cell killing effects in vitro by increased ROS generation	[112]
IR820	TPZ	Glutathione decomposable MSNs (GMONs)	Biocompatibility and stability; GSH/enzyme dual-responsive; tumor targeting by HA	4T1 breast tumor mouse model	Enhanced tumor inhibition rate of dual-loaded nanohybrids was up to 76% under NIR laser irradiation in vivo, due to PDT-induced hypoxia resulting in improved TPZ effects	[113]
Hematop orphyrin (HP)	DOX	CeO_2 NPs coated dual-loaded MSNs (MSN-HP-DOX@CeO_2)	Triple-sensitive (GSH, pH, and light irradiation)	HeLa human cervical carcinoma cells	High cytotoxicity to cancer cells, due to the more controllable DOX release under triple factors	[114]
Si-Pc	DOX	^{68}Ga-labeled magnetic-NIR persistent luminescent hybrid MNPs (DOX/Si-Pc-loaded HMNPs)	Trimodal imaging (NIR-PL, PET, MRI)	Nude mice bearing LNCaP human prostate cancer cells	Outstanding cancer cell killing ability in vitro and tumor suppression effect in vivo, due to prolonged NPs retention and DOX release in tumor area	[115]
Ceramic Nanoparticles (Titanium Oxide Nanoparticles)						
Au@TiO_2 NPs	DOX	Zwitterionic polymer-gated Au@TiO_2 core-	NIR-sensitive; MRI imaging; improved hemocompatibili	Nude mice bearing HeLa human cervical carcinoma	Both in vitro and in vivo anticancer experiments demonstrated that the tumor was effectively	[116]

		shell nanoparticles	ty of NPs; prolonged circulation time.		inhibited, with few side-effects	
ZnPc	Chloram bucil (CBL)	TiO2 nanoparticles ($mTiO_2$-BCBL@ZnPC NPs)	NIR-triggered; ROS-triggered; intratumoral self-sufficiency of O_2	MCF-7 human breast cancer cells	High cytotoxicity effect for cancer cells in vitro due to higher cellular internalization and induction of ROS generation	[91]
TiO_2	DOX	Mesoporous TiO_2 ADH-1-HA-MTN/DOX NPs	Tumor dual targeting by CD44 and N-cadherin; irradiation by X-ray	A549 human non-small-cell lung carcinoma cell line	Enhanced cancer cell killing effects and cell inhibition rate in vitro by increased ROS generation; potential to overcome drug resistance problem by preventing EMT process	[90]
Magnetic Nanoparticles						
Si-Pc	DOX	^{68}Ga-labeled magnetic-NIR persistent luminescent hybrid MNPs (DOX/Si-Pc-loaded HMNPs)	Trimodal imaging (NIR-PL, PET, MRI)	Nude mice bearing LNCaP human prostate cancer cells	Studies with mice tumor models demonstrated that the NP-based combination possessed excellent cancer cell killing ability and an outstanding tumor suppression effect without systemic toxicity, which is associated with prolonged tumor retention of NPs and the durable release of loaded DOX within tumor tissues	[115]
CuS NPs	DOX	Hollow mesoporous CuS NPs capped with magnetic iron oxide NPs (HMCuS/DOX @IONP-PEG)	Controlled drug release; magnetic targeting; property and MR imaging	Nude mice bearing MCF-7 human breast cancer cells	Improved treatment efficiency due to increased drug levels at tumor site and elevated cellular ROS level in vivo; reduced cardiotoxicity of DOX in NPs than free drug	[117]
ICG	Pt (IV) prodrugs	MoS_2 nanoflowers (MoS_2@Fe_3O_4-ICG/Pt (IV))	Trimodal imaging (MR, IR, PA)	L929 fibroblast cells or Hela cells, H22 live cancer mouse model	Enhanced anti-tumor efficacy by both in vitro and in vivo assays	[118]
Ce6	Celastrol (CSL)	Manganese/iron-based nanoprobes (Fe_3O_4@MnO_2-CSL/Ce6)	pH-responsive; intratumoral self-sufficiency of O_2; T1/T2 MRI and PA imaging	Nude mice bearing Bel-7402 human hepatocellular carcinoma cells	Synergistic therapeutic effects for tumor inhibition through improving the tumor hypoxic environment, thereby enhancing PDT effects	[119]

ICG	DOX	MnO_2-coated silk fibroin NPs (SF@MnO_2/ICG/DOX)	Intratumoral self-sufficiency of O_2; dual imaging (FL and MRI)	4T1 breast tumor mouse model	Significant tumor inhibitive efficacy, with a tumor growth inhibition rate of 89.6%, compared to moderate tumor inhibition effect of single therapies at 14 days; H&E staining, TUNEL assays, Ki67, DHE, and HIF-α IF staining of the excised tumor sections were subsequently performed, in order to evaluate the tumor tissue destruction	[120]
Calcium Carbonate Nanoparticles						
ICG	TPZ	Hybrid $CaCO_3$/TPGS nanoparticles	Tumor targeting by RGD peptide	Subcutaneous U87MG and orthotopic B16F10 tumor-bearing mouse model	Intensive effects in vitro and in tumor inhibition, with negligible side-effects	[121]
Metal-Organic Framework-Based PDT plus Chemotherapy						
Porphyrin	DOX	ZnO-gated porphyrinic MOF-AS1411	pH-sensitive; Tumor targeting by nucleolin-specific AS1411 aptamer	Nude mice bearing human HeLa human cervical carcinoma cells	Highly efficient cancer cell killing and tumor inhibition; tumor ablation was also even achieved, without undesirable side-effects	[122]
RuII polypyridyl alkyne complex (Ra)	DOX	UiO-Ra-DOX-CuS	pH-sensitive; NIR-triggered drug release; intratumoral self-sufficiency of O_2	MDA-MB-231 human breast cancer cells	Improved cytotoxicity for cancer cells in vitro than chemotherapy alone (69% vs. 42%)	[123]
Photochlor (HPPH)	AQ4N	Azido-/PS-terminated UiO-66-H/N3 NMOFs	Hypoxia-triggered; enhanced dispersion by PEG layer	Nude mice bearing U87MG human glioblastoma cancer	Enhanced therapeutic efficacy with negligible systemic toxicity due to PDT and hypoxia-activated cytotoxicity of AQ4N	[124]
Ce6	Gambogic acid (GA)	MnO_2-based core-shell GC@MCS NPs	Hypoxia-triggered; intratumoral self-sufficiency of O_2; increased penetration; tumor-targeting by HA	4T1 mammary tumor models	Superior potency and efficacy in tumor regression; 92.41% of 4T1 tumor inhibition rate	[125]
Au@TiO_2 NPs	DOX	Polymer-gated Au@TiO_2 core-shell nanoparticles	NIR-sensitive; MRI imaging; improved hemocompatibility of NPs;	Nude mice bearing HeLa human cervical carcinoma	Both in vitro and in vivo anticancer experiments demonstrated the tumor was effectively inhibited, with minimal side-effects, by the multifunctional NPs	[116]

			prolonged circulation time			
ICG	TPZ	Zeolitic imidazolate framework-8 (ZIF-8) coated ZnS NPs (ZSZIT)	Hypoxia-activated; H_2S-sensitive cascade	Nude mice bearing Huh7 human hepatoma	Synergistic anti-tumor effect both in vitro (by CCK8 assay) and in vivo (by tumor volume change)	[126]
Other Inorganic Nanoparticles						
octaethyl porphine (OEP)	Cis-$(PEt_3)_2Pt(OTf)_2$ (cPt)	Metallacage-loaded NPs	Tumor targeting by cRGDfK; enhanced tumor accumulation and cellular internalization ability	Nude mice bearing A2780/A2780CIS ovarian tumor	Highest anti-tumor outcome, with 89.2% tumor inhibition rate, compared to 14.1%, 25.5%, and 66.8% for chemo, NP-chemo, and NP-PDT, respectively; decreased the hepatotoxicity and nephrotoxicity of the platinum-based anticancer drug	[127]
TPP	Cis-$(PEt_3)_2Pt(OTf)_2$ (cPt)	Metallacage-loaded NPs	Enhanced penetration into drug-resistant 3D tumor spheroids	HuH7 human hepatocellular carcinoma cells and CCLP-1 intrahepatic cancer cells	Enhanced ability to decrease tumor cell mobility and sphenoid formation; CSCs from these spheroids have a lower tumorigenicity, compared to CSCs in the spheroids after single therapy	[128]
ICG	DOX	Hollow mesoporous Prussian blue (HMPB)@PEI/ICG/DOX)	FL imaging due to ICG	4T1 tumor-bearing mouse models	Effective tumor inhibition effect with a tumor growth inhibition rate of 95.5%, while single therapies did not effectively suppress tumor growth in the long term; insignificant short-term toxicity or damage to normal tissues	[129]
NPs	DOX	Hollow CuS nanocubes (CuS@PEG)	NIR-triggered; pH-sensitive	HepG2 human hepatocyte carcinoma cells	Enhanced specific cytotoxicity to cancer cells in vitro	[130]
NPs	DOX	Silver NPs	pH-sensitive; intracellularly probed; tumor targeting by FA	SKOV-3 and L1210 cells	Enhanced toxicity in vitro	[131]

Nanoparticle-Based PDT Plus Immunotherapy

Cancer immunotherapy has been widely explored, both alone and in combination with other therapies. The US Food and Drug Administration (FDA) has approved it for nearly 20 different types of cancer treatments, due to its durable and robust effects. Immunotherapy can be classified into five distinct strategies: nonspecific immune

stimulation (cytokines, Toll-like receptors (TLRs) ligands), vaccination, adoptive cell transfer, checkpoint blockade, and tumor antigen-antibody targeting (Figure 3). A nano technique-based combination of PDT and immunotherapy can improve the therapeutic ratio, prevent drug leakage, and minimize the shortcomings of a single modality [132].

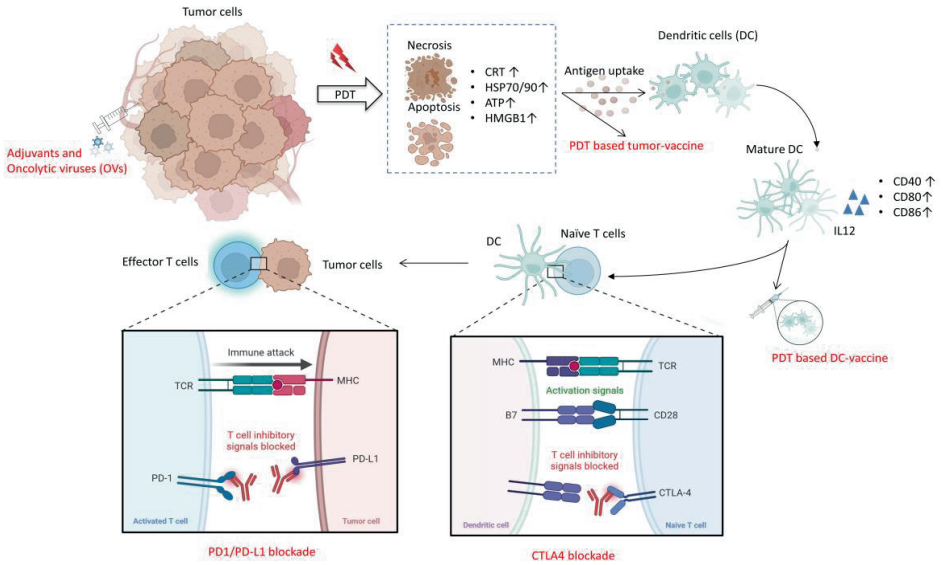

Figure 3. NP-mediated photodynamic therapy in combination with various immune therapies, including vaccination, immune checkpoint inhibitors, oncolytic viruses (OVs), and adjuvants. The combination works to enhance the key factors of the immune-oncology cycle—antigen release, antigen presentation, APC activation, T-cell activation, T-cell infiltration, and antigen recognition—to kill primary tumor cells and overcome tumor recurrence and metastases.

Integrating PDT with immunotherapy in nanoparticles (Table 3) enables the eradication of both the primary tumor and the metastatic cancer cell growth. During treatment, PDT first effectively clears the primary tumor(s) by inducing immunogenic cell death. Subsequently, PDT-induced dying tumor cells are regarded as new tumor-derived antigens, which can be phagocytosed by macrophages and dendritic cells. In addition, increased stress protein expression and DAMP release from tumor cells lead to acute inflammation and leukocyte infiltration, as well as maturation activation of dendritic cells. However, some studies have shown that these series of immune responses are insufficient to inhibit escaped tumor cells. Myeloid-derived suppressor cells (MDSCs) infiltrate the tumor, release anti-inflammatory cytokines, and activate regulatory T cells (Tregs) to inhibit the anti-tumor immune response. Thus, the escaped tumor cells can survive and recover again [133]. In addition to PDT-induced anti-tumor immunity, nanoparticle-based combined photo-immunotherapy can modulate the immune system against survival/metastatic tumor cells, by decreasing immunoregulatory suppression (immune checkpoint blockade therapy) or increasing immunogenicity of the tumor microenvironment (utilizing immunoadjuvants), eventually attracting more antigen-presenting dendritic cells [12].

Table 3. Preclinical studies on PDT plus immunotherapy.

PS	Therapeutic Agents	Delivery System	Therapeutic Outcomes of Combination	Cancer Models	Cytokines	Immune cells	Ref
BPD-MA	Anti-PD1 post NP-based PDT	Poly (ethylene glycol)-modified metal-organic nanoparticles	Enhanced anti-tumor efficacy for primary tumor; inhibitory effects on lung metastasis	4T1 murine breast cancer cells	ND	$CD8^+$ T cells	[134]
Ce6	Codelivery with DOX to generate in situ Vaccine	Cancer cell membrane (CCM)-coated calcium carbonate (CC) nanoparticles	Enhanced ICD; effective inhibition of both primary and distant growth with low-dose PDT and chemotherapy	4T1 murine breast tumor model	IL-6, IL-12, TNF-α	ND	[135]
	In situ vaccine	Lipid (Li)-coated calcium carbonate (CC) vehicle (Li/CC)	Enhanced inhibitory effects on primary and distant tumor growth	Colorectal cancer	-	-	[136]
	Autologous tumor cell-based vaccines	Fmoc-KCRGDK-phenylboronic acid (FK-PBA) hydrogel	Efficiently inhibited tumor relapse	B16-OVA, CT26	TNF-α, IFN-γ	DCs, Treg $CD4^+/CD8^+$ T cells	[137]
	Codelivery with CpG ODNs to generate in situ vaccine	Mesoporous silica nanoparticles	Enhanced immunogenic cell death; effective accumulation of bMSN in tumors (up to 9.0% ID/g) after intravenous administration; enhanced anti-tumor efficacy against locally treated tumors and distant, untreated tumors	MC38 murine colorectal tumor model, B16F10 murine tumor model	IFN-γ	$CD8^+$ T cells, DCs	[138]
	In situ vaccine and further anti-PD1 treatment	PDA@UCNP-PEG/Ce6	Strong anti-tumor immune responses; enhanced anti-tumor efficacy for primary tumor; inhibitory effects on disseminated tumor growth; inhibitory effects on tumor relapse and metastasis	B16F10c, 4T1 murine tumor model	ND	DCs, $CD4^+/CD8^+$ T cells, memory T cells	[139]
	Codelivery with R837 to generate in situ vaccine and then anti-CTLA4 treatment	UCNP-Ce6-R837 nanoparticles	Strong anti-tumor immune responses; enhanced anti-tumor efficacy for primary tumor; inhibitory effects on distant tumor growth; prevented tumor recurrence through a long-term immune memory function	CT26 murine colorectal tumor model	IL-12, IFN-γ, TNF-α	DCs, $CD4^+/CD8^+$ T cells, memory T cells	[140]
	Anti-CTLA4 treatment	CM@M-MON@Ce6 nanoparticles	Enhanced ICD; notable eradication of primary and deeply metastatic tumors	MCF-7 murine breast	TNF-α, IFN-γ,	DCs, $CD4^+/CD8^+$ T cells, CTLs	[141]

	post NP-based PDT			tumor model	IL-6	
	Codelivery with R837 to generate In situ vaccine and then anti-CTLA4 treatment	Ce6-CAT/PEGDA hybrid hydrogel	Enhanced anti-tumor efficacy by means of one injection followed by repeated stimulations; inhibitory effects on distant tumor growth; prevented tumor recurrence through a long-term immune memory function	4T1 murine breast tumor model	IFN-γ, TNF-α	DCs, $CD4^+/CD8^+$ T-cells, memory T cells, Tregs, myeloid-derived suppressor cells [142]
	Anti-PD1 treatment post NP-based PDT	PDA@UCNP-PEG/Ce6	Strong anti-tumor immune responses; enhanced anti-tumor efficacy for primary tumor; inhibitory effects on disseminated tumor growth; inhibitory effects on tumor relapse and metastasis	B16F10c, 4T1 murine breast tumor mice model	ND	DCs, $CD4^+/CD8^+$ T cells, memory T cells [139]
	Anti-PDL1 treatment post NP-based PDT	H-MnO_2-PEG/C&D nanoparticles	Strong anti-tumor immune responses; enhanced combating effects of the primary tumor progression; inhibitory effects on untreated distant tumors	4T1 murine breast tumor model	IL12, IFN-γ, TNF-α	Macrophage, cytotoxic T lymphocytes [143]
	Anti-PDL1 treatment post NP-based PDT	Ce6/MLT@SAB nanoparticles	Improved levels of ICD and abilities to activate dendritic cells in vitro; enhanced PDT killing efficiency in vitro by NPs; augmented anti-tumor effects	4T1 murine breast tumor model	ND	DCs, $CD4^+/CD8^+$ T cells, myeloid-derived suppressor cells [144]
	Codelivery with DOX and then treatment with anti-PDL1	Hybrid TKHNP-C/D nanoparticles	Evoked anticancer immune responses; enhanced inhibition of primary and distant tumor growth	4T1 murine breast tumor model	TNF-α, IFN-γ	DCs, $CD8^+$ T cells, CTLs [145]
Cu-doped carbon dots (CDs)	Anti-PDL1 therapy and starving-like therapy after NP-based PDT	γ-PGA@GOx@Mn, Cu-CDs nanoparticles	Improved treatment efficiency; inhibitory effects on nonirradiated tumors due to systematic anti-tumor immune response	4T1 murine breast tumor model	IFN-γ	CTLs, DCs [146]
HPPH	Codelivery with Dox to generate in situ vaccine	Chimeric crosslinked polymersomes	Enhanced immunogenic cell death; increased mature DCs in tumor-draining lymph nodes (tdLNs) and $CD8^+$ T cells in tumor tissues; enhanced inhibitory effects	MC38 murine colorectal tumor model	IL6	$CD8^+$ T-cells, DCs [147]

			on primary and distant tumor growth				
	In situ vaccine	Graphene (HPPH)-PEGylated GO NPs conjugated with an HK peptide	Effectively ablated primary tumors and destroyed residual tumor cells with SPECT/CT imaging capability; enhanced anti-tumor immunity and immune memory, which help to prevent distant lung metastasis	4T1 murine breast tumor model	IFN-γ	$CD8^+$ T cells, DCs	[148]
H2TCPP	Codelivery with CpG ODNs; in situ vaccine	PCN-ACF-CpG@HA metal-organic nanoparticles	Enhanced immunogenic cell death; effective inhibition of both primary and HIF-1α-induced survival and metastasis	H22 murine hepatic carcinoma cells	TNF-α, IFN-γ, IL-12	DCs	[149]
ICG	Codelivery with siRNA PD-L1	Mn@CaCO3/ICG nanoparticles	Efficient delivery of the loaded drug to the tumor tissues; improved tumor hypoxia; roused the immune system	Lewis lung tumor cells	TNF-γ, INF-γ, IL-12, IL-18	DCs, $CD4^+/CD8^+$ T cells	[150]
	Codelivery with R837 and then treat with anti- CTLA4	PLGA-ICG-R837 nanoparticles	Generated more tumor-associated antigens; generated immunological responses will be able to attack remaining tumor cells in mice, which is useful in metastasis inhibition	4T1 murine breast tumor model, CT26 murine colorectal tumor model	IL-12, IL-1β, IL-6, TNF-α, IFN-γ	DCs, $CD4^+/CD8^+$ T cells, memory T cells	[151]
Porphyrin	Codelivery with cetuximab, further treatment with anti-PDL1	EGFR-CPIG liposomal nanohybrid cerasomes	Enhanced anti-tumor efficacy	CT26 murine colorectal cancer	-	-	[152]
PpIX	Codelivery with CpG ODNs and then anti-PD-L1 therapy	Cu9S5@mSiO₂-PpIX@MnO₂ (CSPM) nanoparticles	Notable eradication of primary tumor; Further combined with PD-L1 blockade therapy, showed potential to inhibit metastasis of tumors	4T1 murine breast tumor model	TNF-α, IFN-γ, IL-12	$CD8^+$ T-cells, CTLs	[153]
Pyropheophorbide	Codelivery with oxaliplatin to generate in situ vaccine, then	NCP@pyrolipid core-shell nanoparticles	Enhanced immunogenic cell death and immunity of PDT; regression of primary tumors and distant tumors in bilateral syngeneic mouse	CT26 and MC38 murine colorectal tumor models	IFN-γ, TNF-α	$CD4^+/CD8^+$ T cells	[154]

	combined with anti-PDL1						
Pyropid	Anti-PDL1 treatment after NP-based PDT	ZnP@pyro nanoparticle	NP-PDT sensitized tumors to checkpoint blockade therapy; enhanced inhibition of primary tumor growth and untreated distant tumors; prevented metastasis to the lung	4T1 murine breast tumor model	IL-6, IFN-γ, TNF-α	Macrophages, DCs	[155]
ZnPc	Codelivery with CpG ODNs	CpG-ODN-Au-ZnPc-poly gold nanoparticles	Increased toxicity of NP-combined therapy than single treatment in vitro; enhanced cytokine levels	4T1 murine breast cancer cells	IL-2, IL-4, IL-6, IL-10, IL-12, TNF-α, IFN-γ	DCs	[156]
Sinoporphyrin sodium (DVDMS)	Codelivery with PD-1 protein by coating onto NP surface (substituting for Anti-PD1)	Human serum albumin (HSA)-perfluorotributylamine @HSA-DVDMS@PD-1 membrane, PHD@PM	Enhanced anti-tumor efficacy (maturation of DCs and tumor infiltration of CTLs)	4T1 murine breast tumor model	TNFαIL10	DCs, CTLs, Th cells, Tregs	[157]
5,10,15,20-Tetra-(4-aminophenyl) porphyrin	Anti-PDL1 treatment post NP-based chemo-PDT	Copper-doped nanoscale covalent organic polymer	Inhibited tumor growth and activated immune responses; suppressed distant tumor growth and cancer metastasis	CT26 murine colorectal tumor models	INF -γ, TNF-α	DCs, CTLs, $CD4^+/CD8^+$ T-cells	[158]

Nanoparticle-Based PDT Plus Immune Checkpoint Blockade Therapy

Nanotechnology-supported PDT combined with immune checkpoint therapy, including anti-PD-1/PD-L1 and anti-CTLA-4, has been reported to have synergistic anti-tumor effects [159]. Nanoparticles have been proposed to decrease the required therapeutic doses, minimize the risk of serious systemic toxicity, and prolong the immune response [160]; for example, it has been demonstrated that loading anti-CTLA-4 monoclonal antibodies in hydrogel micelles [161] or PEGylated liposomes [162] decreased the associated toxicity in healthy organs.

Additionally, PS-based nanoparticles plus immune checkpoint inhibitors are capable of switching off the inhibitory anti-tumor pathways between T cells and tumor cells and normalizing the suppressive tumor microenvironment state. NPs help to enhance the PDT-induced immunomodulation at the same time with PDT, thereby

facilitating complete tumor ablation and inhibiting tumor relapses and metastasis. Zheng et al. generated a novel Janus nanoparticle that combined PDT and magnetic hyperthermia, a type of thermal cancer treatment using magnetic nanoparticles to generate heat [163] while performing a CTLA4 blockade. These nanoparticles improved the levels of ICD and significantly decreased primary tumor weights and the number of pulmonary metastatic nodules in MCF-7 tumor-bearing mice [141].

NP-based PDT combination with commonly used immune checkpoint inhibitors, including anti-PD1 or anti-PD-L1 antibody, shows the potential to inhibit the dissemination of tumor, its relapse, and metastasis by enhancing systemic anti-tumor immune responses. Yan et al. utilized polydopamine-encapsulated UCNPs with surface-loaded PS (Ce6), which significantly enhanced the anti-tumor efficacy of PDT in the primary tumor and prolonged survival time of a 4T1 tumor-bearing mouse model. In addition, combined PDT and PTT therapy using these NPs enhanced ICD levels and systemic anti-tumor immune responses. The effect was further improved by the combination with anti-PD1 antibody, through the enhanced activity of macrophages, B cells, $CD4^+/CD8^+$ T cells, IFN-γ-expressing CTLs, and effector memory T-cells [139]. Another study, which used both 4T1 and TUBO (a cloned BALB-neuT mouse mammary carcinoma cell line) bilateral syngeneic mouse models, showed that combined NP-mediated PDT with PD-L1 antibody completely eradicated the tumor, and there was a low (0.4%) metastasis rate of tumor nodules in the lungs [155].

Nanoparticle-Based PDT Plus Vaccination and Immunoadjuvants

Therapeutic cancer vaccines are based on targeting specific tumor-associated antigens (TAA) and adjuvants, in order to enhance the cancer antigen presentation of antigen-presenting cells (APCs) and the activation of T cells [164]. As shown in Figure 4, in the context of PDT-immuno-vaccine therapy, studies have focused on the systemic delivery of PDT-treated tumor cell debris as antigens and/or immunoadjuvants, defined as conventional vaccines. Moreover, accumulated NPs loaded with PS and adjuvants have been reported to induce a strong ICD by providing irradiation as an in situ cancer vaccine [165].

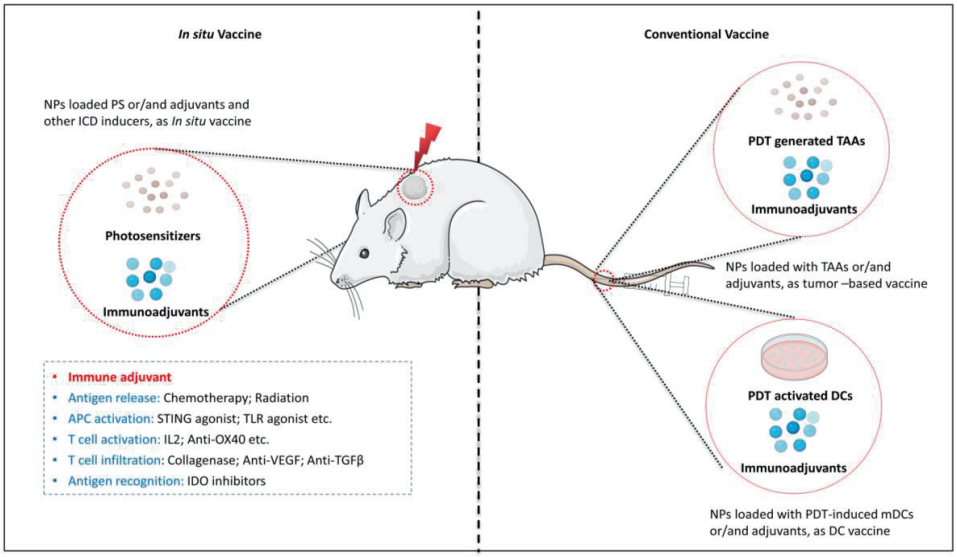

Figure 4. Nanoparticle-based PDT generated vaccines: (**a**) NPs carrying PS and/or immune adjuvants accumulate in tumor tissue after administration. Through irradiation, PDT itself will supply tumor antigens; (**b**) NPs carrying PDT-generated tumor antigens or ex vivo stimulated mature DCs (and/or together with immune adjuvant) are administered systemically as conventional vaccines. This activates and expands effector T cells for vaccine antigen-specific systemic responses. With the help of immune adjuvants and other ICD inducers, strong systemic antitumor immunity against all tumor antigens will be induced, and PDT treatment will ablate surviving tumor cells and metastatic cells.

Nanoparticle-based PDT-Generated Conventional Vaccines

Regarding PDT-generated tumor cell vaccines, tumor cells are treated by PDT ex vivo to induce necrosis and apoptosis. This leads to an increased expression of heat-shock proteins on the tumor cell surface and the generation of neo antigen specific antigens [166]. Thus, they may have the ability to fight the same tumor or tumors with inherent low immunogenicity [6,167]. The anticancer efficiency of vaccines can be further enhanced by appropriate drug delivery systems and adjuvants. NPs protect antigens from rapid degradation or elimination before they achieve their robust and long-term therapeutic effects. For example, a hydrogel-delivered PDT-tumor cell vaccine successfully delayed tumor growth kinetics and prevented the relapse of tumors. Weak bioluminescence signals in lungs and apoptosis/necrosis in collapsed tumor tissues by H&E staining were detected in the hydrogel-based vaccine group. These results demonstrated that the hydrogel vaccine cooperating with PDT induced stronger anti-tumor immunity than PDT alone [137]. Interestingly, it has been reported that the quality of a PDT-based tumor cell vaccine is also affected by other factors; for example, regulatory macrophages (Mregs, anti-inflammatory macrophages subset) impeded the anti-tumor immune response activation by a temoporfin-PDT-/Ce6-PDT-mediated vaccine—these kinds of vaccines are generated using PDT-treated tumor cells as antigens to stimulate the immune system to

kill the cancer cells. However, it has been shown that the inhibitory anticancer effect of Mregs can be relieved through the use of antibodies with Mreg immunodepleting properties (e.g., anti GR1 antibody) in squamous cell carcinoma SCCVII tumor models [168,169]. On the basis of such explorations, it is possible to design and prepare nanoparticles combined with inhibitors or antibodies, in order to generate better PDT-based tumor cell vaccines in the future.

In addition to PDT-generated tumor cell vaccines, investigators developed a PDT-induced therapeutic dendritic cell (DC) vaccination by tumor-specifically triggering DC activation and IL12 expression [170]. They immunized SKH-1 mice with DCs after stimulation by PDT-treated PECA cells. A complete inhibition of tumors was observed in the PDT-DC vaccine group at 21 days after rechallenging vaccinated mice with the same PECA tumor cells.

The combination of PDT with other conventional vaccines (e.g., peptide and genetic vaccines), such as TLR5 agonist flagellin-adjuvanted tumor-specific peptide vaccination (FlaB-Vax) has revealed that this combination can enhance the infiltration of antigen-specific $CD8^+$ T cells, effector memory $CD8^+$ T cells, and IFN-γ expression in a B16-F10 tumor-bearing model [171]. Furthermore, combination treatment of PDT with a synthetic long peptide (SLP) vaccine, covering T-cell (CD4 and CD8) epitopes of tumor antigens (i.e., from the human papillomavirus (HPV)16 E7 oncoprotein), has been regarded as a prospective treatment method for oncogenic virus-induced cancers (e.g., HPV or leukemia virus). This has been proven in murine TC-1 and RMA tumor models by enhanced local tumor ablation and robust systemic immune responses after combination therapy of SLP vaccine and PDT [172].

Nanoparticle-Based PDT-Induced in Situ Vaccines

In addition to these conventional vaccination strategies, PDT has a vaccine effect in situ, due to the induced ICD. In peritoneal mesothelioma, a study has shown that a PDT-induced in situ DC vaccine led to highly significant survival in vivo. Moreover, the anti-tumor immune responses of the vaccine were enhanced when combined with CTLA4 blockade. In particular, this combined treatment regimen stimulated the proliferation, cytotoxic effects, and activation of $CD4^+$/$CD8^+$ T cells, with a more rapid migration toward the lymph nodes than a traditional LPS-induced DC vaccine [173]. Furthermore, a combination of ICD-inducing therapies (chemotherapy and radiotherapy) with nanoparticles greatly improved the immunogenicity and downstream immune responses of the PDT-induced immune vaccine. For example, a nanoscale chimeric crosslinked polymersome (CCPS) composed of PS and DOX for TAA secretion to produce in situ DC vaccination showed better MC38 tumor growth inhibition and lower distant tumor formation due to DC activation enhancement by CCPS and PDT [147]. Another innovative discovery was the combined intervention of an oncolytic viral vaccine (in situ vaccine) and protoporphyrin IX (PpIX)-mediated PDT. This resulted in complete cell death in a human pancreatic cancer cell line (PsPC-1 and BXPC-3), when compared to 30% single PDT-induced cell death [174].

Additionally, NPs themselves can intrinsically stimulate immune responses as adjuvants, such as positively charged polymers containing primary, secondary, or tertiary amines. Yang et al. reported a chimeric crosslinked polymersome acting as an adjuvant

by inducing proinflammation factor release and activating the stimulator of interferon genes (STING)-dependent pathway. The system simultaneously combined PDT, DC vaccine, and chemotherapy (DOX). It enhanced the tumor abscopal effect in primary and distant colon MC38 tumors by increasing DC maturation in lymph nodes and $CD8^+$ T cells in the tumor(s) [147]. Taken together, PDT combined vaccines are an effective way to induce host immunity against the primary tumor and tumor relapse; as such, they are currently being assessed in both preclinical and clinical trials.

Enhanced Vaccination Effects by Immunoadjuvants in Nanoparticles

Similar to antigens, the limitations of adjuvants include rapid degradation, clearance, and ineffective cellular uptake. Nanoparticles supporting vaccines can load PS and immunoadjuvants synchronously, in order to minimize systemic side-effects and to enhance the anti-tumor efficacy of the two therapies [175]. The immunopotentiators in the nanosystems may enhance the PDT-induced immune responses by targeting APCs and acting as in situ vaccines to modulate tumor growth. There are various adjuvants in cancer immunotherapy, defined as immunotherapeutic agents targeting tumor cells, T cells, and ligands for pattern recognition receptors (PRR), which have been reported to induce immune responses [176].

Some commonly used APC-targeting immunoadjuvants in clinical practice have been successfully tested to act as partners to PDT. Imiquimod (R837) has the capability to activate DCs and B cells to induce cytokines for Th1 cell immunity and facilitate antibody production [177]. Xu et al. synthesized multitasking UCNP-Ce6-R837 nanoparticles. This nanoparticle triggered robust immune responses, including enhanced DC activation, enriched effective T-cell population, and long-term immune memory, to inhibit primary and distant tumor growth and to prevent tumor recurrence [140]. Notably, PDT treatment of large established tumors enhances the uptake of NPs in the tumor, which accumulates in the myeloid cells in the tumor microenvironment [178]. Moreover, PDT combined with intratumoral injection of immunostimulatory NPs encapsulated with TLR3-/TLR7-ligands and chemotactic agent MIP3alpha synergizes in local and distant antitumor effects [179]. In addition, a chitosan-derived immunoadjuvant has been shown to synergistically enhance the immune response during PDT irradiation [180]. CpG oligodeoxynucleotides (ODNs) contain unmethylated CpG motifs, which can boost immune responses (e.g., DC activation and local inflammation) after PDT, by triggering cells that express Toll-like receptor 9, including dendritic cells and B cells [181]. Cai et al. reported metal-organic framework (MOF)-based nanoparticles coloaded with PS and CpG adjuvant. This nanoparticle strongly enhanced the level of TAAs and led to in situ DC vaccination, in order to inhibit primary tumor growth, HIF-1α-induced survival, and metastasis in a H22 mouse model [150]. Zhang et al. utilized pH-responsive metallic core-shell composite nanoparticles consisting of copper sulfide coated with a mesoporous silica ($mSiO_2$) shell, CpG ODNs, and PS (PpIX). In addition, the NP-based combination showed remarkable anticancer effects by overcoming the limitation of the hypoxia tumor environment due to PDT anti-tumor efficacy (MnO_2 can decompose PDT-generated H_2O_2 into oxygen) and enhanced CTL infiltration and IFN-γ production by CpG ODNs in the tumor. Furthermore, their results showed that this NP, when combined with PD-L1 blockade therapy, has the potential to inhibit metastasis of tumors [154]. Several other

APC-targeting immunoadjuvants may work as promising therapeutic supporters for PDT, such as TLR2 agonists (CL401/CL413/CL429), an activator of the proinflammatory transcription factor NF-κB (Pam3CSK4), and agonists of the stimulator of IFN genes (STING). Significant efforts are required to explore the combination with PDT for personalized therapy design.

Moreover, the combination of PDT and T-cell activators which intensify the direct activation of T cells (e.g., anti-OX40, IL-2, and anti-CD3/28) or therapeutic cargoes affecting T-cell infiltration into tumor tissues (e.g., collagenase, anti-VEGF, and anti-transforming growth factor (TGF-β) is also a promising strategy to improve the treatment efficiency. David et al. showed that T cells activated by anti-CD3 and anti-CD28 antibodies display an increased sensitivity to Pc4-PDT-induced apoptosis (10.6-81.2%), indicating the potential of combining PDT with T-cell agonists [182]. Ling et al. constructed hollow mesoporous organosilica nanoparticles (HMONs) encapsulated with collagenase (Col); they could degrade the collagen I fiber in the extracellular matrix (ECM) to normalize the tumor immune suppression environment, before being hybridized with the PS HPPH. Nanoparticle HMONs have been employed as delivery systems with excellent loading capacity, biocompatibility, and biodegradability. They were shown to have better anti-tumor effects in a tumor mouse model than PDT alone. Immunofluorescence characterization of tumor tissues demonstrated the degradation of ECM after treatment, which was linked to increased immune response and O_2 infiltration into tumor tissues [183]. More agents that target T-cell infiltration combined with PDT were discussed in a previous section (targeted therapy). Taken together, studies that focus on PDT combined with immunologic adjuvants are currently limited, and it will be worthwhile to further explore these as novel treatment options.

PDT Plus Nonspecific Immune Stimulation

Cytokines have proven to be a novel therapeutic approach in treating patients with advanced malignancies. Interferon-γ (IFN-γ), interferon-α (IFN-α), interleukin-2 (IL2), tumor necrosis factor-α (TNFα), and interleukin-12 (IL12) are the most successful therapeutics approved for clinical use. Some of these cytokines have shown enhanced anti-tumor effects when combined with PDT therapy; for instance, PDT in combination with vitamin D3-binding protein-derived macrophage-activating factor (DBPMAF) showed enhanced tumor-inhibitory effects by inhibiting angiogenesis [184]. Moreover, the tumor-controlling effects of PDT were potentiated by the intraperitoneal administration of recombinant human TNF-α in mice [185]. Administration of granulocyte-macrophage colony-stimulating factor (GM-CSF) functioned by increasing macrophage infiltration to enhance PDT-induced effects [186]. However, the relatively high toxicity of cytokine therapy and the complex tumor environment limit its usage in clinical settings. Hence, through the integration of PDT and cytokines in nano-frames, the essence of the two therapies can be achieved, and the shortcomings of cytokine therapy can be mitigated. Cytokines in NPs can generate an optimal immune response to help PDT eradicate both the solid and the metastatic tumor. However, few studies have been performed, and more investigation is warranted to explore how delivery systems assist in combined PDT-cytokine therapy.

Nanoparticle-Based PDT in Cancer Theragnostic

From metal complexes to polymeric nanoparticles, NP-based PDT combination platforms have been employed for multimodal imaging (e.g., magnetic resonance (MRI), photoacoustic (PA), positron emission tomography (PET), and computed tomography (CT)) and diagnosis systems, due to the inherent fluorescence of PSs, the physical properties of NPs, and the use of doped contrast agents (i.e., a medium that can increase the contrast of internal body structures or fluids in medical imaging).

In particular, formulations that are based on AuNPs, superparamagnetic NPs (SPIONs), graphene oxide (GO), and carbon nanodots (CDs), among others, have the potential to combine diagnosis, monitoring, and therapy in the same nanoplatforms [187]. As discussed above, ^{64}Cu-labeled lipoprotein-mimicking NPs could provide preoperative PET/CT imaging for primary tumor localization and intraoperative fluorescence imaging for the visualization of tumors and the subsequent lymphatic drainage network status 24 h after intravenous injection in a VX-2 buccal carcinoma rabbit model [23]. In addition to labeling with ^{64}Cu, ^{18}F, $^{124/125}$I, and ^{125}Cd can act as PET contrast agents for nanoparticles. Moreover, researchers have developed hyaluronic acid-modified Au nanocages (AuNCs-HA), allowing for thermoelastic expansion-induced imaging upon PA waves, thus integrating imaging and RT-PDT therapy into one platform [29]. This may lead to future studies focused on the combination of imaging-guided surgery/RT with PDT.

NPs based on the use of paramagnetic ions (e.g., Gd^{3+}, Mn^{2+}, Dy^{3+}, Fe^{3+}, and Ho^{3+}) have the ability to facilitate MRI imaging [188]; for example, core-shell structured $NaGdF_4$:Yb-UCNPs containing Pt(IV) prodrugs were modified with polyethyleneimine (PEI), conjugated with DSP molecules and $ZnFe_2O_4$-dopamine ($ZnFe_2O_4$-DA) NPs, and subsequently coated with a PEG layer. Therefore, this platform integrates UCL, CT, MRI,

and PA, thus serving as a multimodal bioimaging system [94]. Hybrid metal NPs based on mesoporous silica NPs, integrating NIR-PLNPs ($Ga_2O_3:Cr^{3+}$, Nd^{3+}), magnetic nanoparticles (Gd_2O_3), and radionuclides (^{68}Ga) in one constructor, were named DOX/Si-Pc-loaded HMNPs. This all-in-one system, developed by Rui et al., possesses the advantages of long-term trimodal imaging ability (NIR-PL, PET, and MRI) with the synergistic tumor inhibition effect of chemotherapy and PDT [114], proving an ideal nanoplatform for combination cancer theragnostic and cancer therapy.

Concluding Remarks and Future Outlook

In conclusion, the increasing incidence of patients with advanced cancer, postoperative recurrence, cancer cell metastasis, and the emergence of drug resistance requires alternative treatment options. The insights from the last several years increasingly support the idea that PDT is a powerful strategy for superficial cancer treatment, such as non-melanoma skin cancer, with advantages of minor damage, few side-effects, and precise treatment. However, some inherent shortcomings limit the clinical application of PDT, such as lack of tumor-specific targeting, penetration depth, and tumor microenvironment properties. Here, we review that PDT alone is not effective enough in some hypoxic and deep solid tumors and may be successfully combined with other therapies to enhance efficacy. Many studies show that the application of nanoparticle-based codelivery methods is very promising and can be expected to speed up the success of PDT combined therapy. In separate delivery, PDT also shows the potential to enhance NP accumulation in tumor areas, which will boost the efficiency of NP-loaded therapeutic agents.

However, as most studies focused on in vitro and in vivo mice models, it is necessary to validate these combination strategies in clinical settings. There are some remaining challenges in the current clinical application of NP-based PDT combination therapy: (1) identification of appropriate targets for the complex tumor environment [189]; (2) improvement of entrapment efficiency, particle stability, and controlled release rate of therapeutic agents from NPs. The accurate drug release control of complex NPs structures is required, which leads to expensive assembly costs for scale-up production and slow approval from FDA; (3) the highly heterogeneous and continuously changing tumor microenvironment is another major challenge that needs to be overcome. Further insights that are needed for the clinical translation of the preclinical studies include (a) optimizing the design (including size, charge, shape, targeted ligands on NPs surface, and stimuli-responsive structure) and synthesis methods (including coprecipitation, inert gas condensation, sputtering, and microemulsion) of nanoparticles that is optimal for the specific cancer therapy [190-192], (b) adjusting the targeting and pharmacokinetic behaviors of nanomaterials, in order to improve their safety and efficacy [189], (c) developing more combination strategies to establish precise and personalized treatment, such as the combination of PDT with starvation therapy, gas therapy (nitric oxide (NO)), laser-induced hyperthermia, and ultrasound therapy [193-196]; and (d) exploring the mechanisms behind the different combinations, in order to control potential side-effects. These insights will provide new ground for transiting NP-based PDT combination therapies to future clinical practice. By overcoming these challenges, PDT combination therapy supported by nanotechnology will become a promising cancer treatment strategy and improve clinical benefit for cancer patients.

References

1. Sung, H.; Ferlay, J.; Siegel, R.L.; Laversanne, M.; Soerjomataram, I.; Jemal, A.; Bray, F. Global Cancer Statistics 2020: GLOBOCAN Estimates of Incidence and Mortality Worldwide for 36 Cancers in 185 Countries. *CA Cancer J. Clin.* **2021**, *71*, 209-249, doi:10.3322/caac.21660.
2. Faguet, G.B. A brief history of cancer: Age-old milestones underlying our current knowledge database. *Int. J. Cancer* **2015**, *136*, 2022-2036, doi:10.1002/ijc.29134.
3. Wan, M.T.; Lin, J.Y. Current evidence and applications of photodynamic therapy in dermatology. *Clin. Cosmet. Investig. Dermatol.* **2014**, *7*, 145-163, doi:10.2147/CCID.S35334.
4. Moan, J.; Juzenas, P. Singlet oxygen in photosensitization. *J. Environ. Pathol. Toxicol. Oncol.* **2006**, *25*, 29-50, doi:10.1615/jenvironpatholtoxicoloncol.v25.i1-2.30.
5. Allison, R.R.; Moghissi, K. Photodynamic Therapy (PDT): PDT Mechanisms. *Clin. Endosc.* **2013**, *46*, 24-29, doi:10.5946/ce.2013.46.1.24.
6. Castano, A.P.; Mroz, P.; Hamblin, M.R. Photodynamic therapy and anti-tumour immunity. *Nat. Rev. Cancer* **2006**, *6*, 535-545, doi:10.1038/nrc1894.
7. Agostinis, P.; Berg, K.; Cengel, K.A.; Foster, T.H.; Girotti, A.W.; Gollnick, S.O.; Hahn, S.M.; Hamblin, M.R.; Juzeniene, A.; Kessel, D.; et al. Photodynamic therapy of cancer: An update. *CA Cancer J. Clin.* **2011**, *61*, 250-281, doi:10.3322/caac.20114.
8. Farkona, S.; Diamandis, E.P.; Blasutig, I.M. Cancer immunotherapy: The beginning of the end of cancer? *BMC Med.* **2016**, *14*, 73, doi:10.1186/s12916-016-0623-5.
9. Steeg, P.S. Targeting metastasis. *Nat. Rev. Cancer* **2016**, *16*, 201-218, doi:10.1038/nrc.2016.25.
10. Fares, J.; Fares, M.Y.; Khachfe, H.H.; Salhab, H.A.; Fares, Y. Molecular principles of metastasis: A hallmark of cancer revisited. *Signal Transduct. Target. Ther.* **2020**, *5*, 28, doi:10.1038/s41392-020-0134-x.
11. Housman, G.; Byler, S.; Heerboth, S.; Lapinska, K.; Longacre, M.; Snyder, N.; Sarkar, S. Drug resistance in cancer: An overview. *Cancers* **2014**, *6*, 1769-1792, doi:10.3390/cancers6031769.
12. Vasan, N.; Baselga, J.; Hyman, D.M. A view on drug resistance in cancer. *Nature* **2019**, *575*, 299-309, doi:10.1038/s41586-019-1730-1.
13. Da Silva, C.G.; Peters, G.J.; Ossendorp, F.; Cruz, L.J. The potential of multi-compound nanoparticles to bypass drug resistance in cancer. *Cancer Chemother. Pharmacol.* **2017**, *80*, 881-894, doi:10.1007/s00280-017-3427-1.
14. Jin, F.; Liu, D.; Xu, X.; Ji, J.; Du, Y. Nanomaterials-Based Photodynamic Therapy with Combined Treatment Improves Antitumor Efficacy through Boosting Immunogenic Cell Death. *Int. J. Nanomed.* **2021**, *16*, 4693-4712, doi:10.2147/IJN.S314506.
15. Kwon, N.; Kim, H.; Li, X.; Yoon, J. Supramolecular agents for combination of photodynamic therapy and other treatments. *Chem. Sci.* **2021**, *12*, 7248-7268, doi:10.1039/d1sc01125a.
16. Wang, X.; Ramamurthy, G.; Shirke, A.A.; Walker, E.; Mangadlao, J.; Wang, Z.; Wang, Y.; Shan, L.; Schluchter, M.D.; Dong, Z.; et al. Photodynamic Therapy Is an Effective Adjuvant Therapy for Image-Guided Surgery in Prostate Cancer. *Cancer Res.* **2020**, *80*, 156-162, doi:10.1158/0008-5472.CAN-19-0201.
17. Wang, X.; Tsui, B.; Ramamurthy, G.; Zhang, P.; Meyers, J.; Kenney, M.E.; Kiechle, J.; Ponsky, L.; Basilion, J.P. Theranostic Agents for Photodynamic Therapy of Prostate Cancer by Targeting Prostate-Specific Membrane Antigen. *Mol. Cancer Ther.* **2016**, *15*, 1834-1844, doi:10.1158/1535-7163.MCT-15-0722.
18. Lutje, S.; Heskamp, S.; Franssen, G.M.; Frielink, C.; Kip, A.; Hekman, M.; Fracasso, G.; Colombatti, M.; Herrmann, K.; Boerman, O.C.; et al. Development and characterization of a theranostic multimodal anti-PSMA targeting agent for imaging, surgical guidance, and targeted photodynamic therapy of PSMA-expressing tumors. *Theranostics* **2019**, *9*, 2924-2938, doi:10.7150/thno.35274.

19. Mangadlao, J.D.; Wang, X.; McCleese, C.; Escamilla, M.; Ramamurthy, G.; Wang, Z.; Govande, M.; Basilion, J.P.; Burda, C. Prostate-Specific Membrane Antigen Targeted Gold Nanoparticles for Theranostics of Prostate Cancer. *ACS Nano* **2018**, *12*, 3714-3725, doi:10.1021/acsnano.8b00940.
20. Feng, Y.; Wu, Y.; Zuo, J.; Tu, L.; Que, I.; Chang, Y.; Cruz, L.J.; Chan, A.; Zhang, H. Assembly of upconversion nanophotosensitizer in vivo to achieve scatheless real-time imaging and selective photodynamic therapy. *Biomaterials* **2019**, *201*, 33-41, doi:10.1016/j.biomaterials.2019.02.015.
21. Zuo, J.; Tu, L.; Li, Q.; Feng, Y.; Que, I.; Zhang, Y.; Liu, X.; Xue, B.; Cruz, L.J.; Chang, Y.; et al. Near Infrared Light Sensitive Ultraviolet-Blue Nanophotoswitch for Imaging-Guided "Off-On" Therapy. *ACS Nano* **2018**, *12*, 3217-3225, doi:10.1021/acsnano.7b07393.
22. Jin, G.; He, R.; Liu, Q.; Dong, Y.; Lin, M.; Li, W.; Xu, F. Theranostics of Triple-Negative Breast Cancer Based on Conjugated Polymer Nanoparticles. *ACS Appl. Mater. Interfaces* **2018**, *10*, 10634-10646, doi:10.1021/acsami.7b14603.
23. Muhanna, N.; Cui, L.; Chan, H.; Burgess, L.; Jin, C.S.; MacDonald, T.D.; Huynh, E.; Wang, F.; Chen, J.; Irish, J.C.; et al. Multimodal Image-Guided Surgical and Photodynamic Interventions in Head and Neck Cancer: From Primary Tumor to Metastatic Drainage. *Clin. Cancer Res.* **2016**, *22*, 961-970, doi:10.1158/1078-0432.CCR-15-1235.
24. Wang, H.; Wang, Z.; Chen, W.; Wang, W.; Shi, W.; Chen, J.; Hang, Y.; Song, J.; Xiao, X.; Dai, Z. Self-assembly of photosensitive and radiotherapeutic peptide for combined photodynamic-radio cancer therapy with intracellular delivery of miRNA-139-5p. *Bioorg. Med. Chem.* **2021**, *44*, 116305, doi:10.1016/j.bmc.2021.116305.
25. Liu, J.; Yang, Y.; Zhu, W.; Yi, X.; Dong, Z.; Xu, X.; Chen, M.; Yang, K.; Lu, G.; Jiang, L.; et al. Nanoscale metal-organic frameworks for combined photodynamic & radiation therapy in cancer treatment. *Biomaterials* **2016**, *97*, 1-9, doi:10.1016/j.biomaterials.2016.04.034.
26. Liu, J.; Hu, F.; Wu, M.; Tian, L.; Gong, F.; Zhong, X.; Chen, M.; Liu, Z.; Liu, B. Bioorthogonal Coordination Polymer Nanoparticles with Aggregation-Induced Emission for Deep Tumor-Penetrating Radio- and Radiodynamic Therapy. *Adv. Mater.* **2021**, *33*, e2007888, doi:10.1002/adma.202007888.
27. Schaffer, M.; Schaffer, P.M.; Corti, L.; Gardiman, M.; Sotti, G.; Hofstetter, A.; Jori, G.; Duhmke, E. Photofrin as a specific radiosensitizing agent for tumors: Studies in comparison to other porphyrins, in an experimental in vivo model. *J. Photochem. Photobiol. B* **2002**, *66*, 157-164, doi:10.1016/s1011-1344(02)00237-3.
28. Schaffer, M.; Ertl-Wagner, B.; Schaffer, P.M.; Kulka, U.; Jori, G.; Duhmke, E.; Hofstetter, A. The Application of Photofrin II as a sensitizing agent for ionizing radiation—A new approach in tumor therapy? *Curr. Med. Chem.* **2005**, *12*, 1209-1215, doi:10.2174/0929867053764653.
29. Xu, X.; Chong, Y.; Liu, X.; Fu, H.; Yu, C.; Huang, J.; Zhang, Z. Multifunctional nanotheranostic gold nanocages for photoacoustic imaging guided radio/photodynamic/photothermal synergistic therapy. *Acta Biomater.* **2019**, *84*, 328-338, doi:10.1016/j.actbio.2018.11.043.
30. Wang, G.D.; Nguyen, H.T.; Chen, H.; Cox, P.B.; Wang, L.; Nagata, K.; Hao, Z.; Wang, A.; Li, Z.; Xie, J. X-ray Induced Photodynamic Therapy: A Combination of Radiotherapy and Photodynamic Therapy. *Theranostics* **2016**, *6*, 2295-2305, doi:10.7150/thno.16141.
31. Luksiene, Z.; Kalvelyte, A.; Supino, R. On the combination of photodynamic therapy with ionizing radiation. *J. Photochem. Photobiol. B* **1999**, *52*, 35-42, doi:10.1016/s1011-1344(99)00098-6.
32. Ni, K.; Lan, G.; Chan, C.; Duan, X.; Guo, N.; Veroneau, S.S.; Weichselbaum, R.R.; Lin, W. Ultrathin metal-organic layer-mediated radiotherapy-radiodynamic therapy enhances immunotherapy of metastatic cancers. *Matter* **2019**, *1*, 1331-1353.

33. Lu, K.; He, C.; Guo, N.; Chan, C.; Ni, K.; Lan, G.; Tang, H.; Pelizzari, C.; Fu, Y.X.; Spiotto, M.T.; et al. Low-dose X-ray radiotherapy-radiodynamic therapy via nanoscale metal-organic frameworks enhances checkpoint blockade immunotherapy. *Nat. Biomed. Eng.* **2018**, *2*, 600-610, doi:10.1038/s41551-018-0203-4.
34. Ferrario, A.; von Tiehl, K.F.; Rucker, N.; Schwarz, M.A.; Gill, P.S.; Gomer, C.J. Antiangiogenic treatment enhances photodynamic therapy responsiveness in a mouse mammary carcinoma. *Cancer Res.* **2000**, *60*, 4066-4069.
35. Ferrario, A.; Von Tiehl, K.; Wong, S.; Luna, M.; Gomer, C.J. Cyclooxygenase-2 inhibitor treatment enhances photodynamic therapy-mediated tumor response. *Cancer Res.* **2002**, *62*, 3956-3961.
36. Emens, L.A.; Middleton, G. The interplay of immunotherapy and chemotherapy: Harnessing potential synergies. *Cancer Immunol. Res.* **2015**, *3*, 436-443, doi:10.1158/2326-6066.CIR-15-0064.
37. Luo, D.; Carter, K.A.; Miranda, D.; Lovell, J.F. Chemophototherapy: An Emerging Treatment Option for Solid Tumors. *Adv. Sci.* **2017**, *4*, 1600106, doi:10.1002/advs.201600106.
38. Zhao, C.Y.; Cheng, R.; Yang, Z.; Tian, Z.M. Nanotechnology for Cancer Therapy Based on Chemotherapy. *Molecules* **2018**, *23*, 826,doi:10.3390/molecules23040826.
39. Zhang, Y.; Huang, F.; Ren, C.; Yang, L.; Liu, J.; Cheng, Z.; Chu, L.; Liu, J. Targeted Chemo-Photodynamic Combination Platform Based on the DOX Prodrug Nanoparticles for Enhanced Cancer Therapy. *ACS Appl. Mater. Interfaces* **2017**, *9*, 13016-13028, doi:10.1021/acsami.7b00927.
40. Makadia, H.K.; Siegel, S.J. Poly Lactic-co-Glycolic Acid (PLGA) as Biodegradable Controlled Drug Delivery Carrier. *Polymers* **2011**, *3*, 1377-1397, doi:10.3390/polym3031377.
41. Gaio, E.; Conte, C.; Esposito, D.; Reddi, E.; Quaglia, F.; Moret, F. CD44 Targeting Mediated by Polymeric Nanoparticles and Combination of Chlorine TPCS2a-PDT and Docetaxel-Chemotherapy for Efficient Killing of Breast Differentiated and Stem Cancer Cells In Vitro. *Cancers* **2020**, *12*, 278, doi:10.3390/cancers12020278.
42. Liu, X.L.; Dong, X.; Yang, S.C.; Lai, X.; Liu, H.J.; Gao, Y.; Feng, H.Y.; Zhu, M.H.; Yuan, Y.; Lu, Q.; et al. Biomimetic Liposomal Nanoplatinum for Targeted Cancer Chemophototherapy. *Adv. Sci.* **2021**, *8*, 2003679, doi:10.1002/advs.202003679.
43. Wang, Y.; Xie, Y.; Li, J.; Peng, Z.H.; Sheinin, Y.; Zhou, J.; Oupicky, D. Tumor-Penetrating Nanoparticles for Enhanced Anticancer Activity of Combined Photodynamic and Hypoxia-Activated Therapy. *ACS Nano* **2017**, *11*, 2227-2238, doi:10.1021/acsnano.6b08731.
44. Huang, Z.; Xiao, H.; Lu, X.; Yan, W.; Ji, Z. Enhanced photo/chemo combination efficiency against bladder tumor by encapsulation of DOX and ZnPC into in situ-formed thermosensitive polymer hydrogel. *Int. J. Nanomed.* **2018**, *13*, 7623-7631, doi:10.2147/IJN.S179226.
45. He, H.; Zhu, R.; Sun, W.; Cai, K.; Chen, Y.; Yin, L. Selective cancer treatment via photodynamic sensitization of hypoxia-responsive drug delivery. *Nanoscale* **2018**, *10*, 2856-2865, doi:10.1039/c7nr07677k.
46. Jing, X.; Zhi, Z.; Jin, L.; Wang, F.; Wu, Y.; Wang, D.; Yan, K.; Shao, Y.; Meng, L. pH/redox dual-stimuli-responsive cross-linked polyphosphazene nanoparticles for multimodal imaging-guided chemo-photodynamic therapy. *Nanoscale* **2019**, *11*, 9457-9467, doi:10.1039/c9nr01194c.
47. Hu, D.; Chen, L.; Qu, Y.; Peng, J.; Chu, B.; Shi, K.; Hao, Y.; Zhong, L.; Wang, M.; Qian, Z. Oxygen-Generating Hybrid Polymeric Nanoparticles with Encapsulated Doxorubicin and Chlorin e6 for Trimodal Imaging-Guided Combined Chemo-Photodynamic Therapy. *Theranostics* **2018**, *8*, 1558-1574, doi:10.7150/thno.22989.
48. Hao, Y.; Chen, Y.; He, X.; Yu, Y.; Han, R.; Li, Y.; Yang, C.; Hu, D.; Qian, Z. Polymeric Nanoparticles with ROS-Responsive Prodrug and Platinum Nanozyme for Enhanced Chemophotodynamic Therapy of Colon Cancer. *Adv. Sci.* **2020**, *7*, 2001853, doi:10.1002/advs.202001853.

49. Luo, Z.; Li, M.; Zhou, M.; Li, H.; Chen, Y.; Ren, X.; Dai, Y. O2-evolving and ROS-activable nanoparticles for treatment of multi-drug resistant Cancer by combination of photodynamic therapy and chemotherapy. *Nanomedicine* **2019**, *19*, 49-57, doi:10.1016/j.nano.2019.03.007.
50. Gaio, E.; Conte, C.; Esposito, D.; Miotto, G.; Quaglia, F.; Moret, F.; Reddi, E. Co-delivery of Docetaxel and Disulfonate Tetraphenyl Chlorin in One Nanoparticle Produces Strong Synergism between Chemo- and Photodynamic Therapy in Drug-Sensitive and -Resistant Cancer Cells. *Mol. Pharm.* **2018**, *15*, 4599-4611, doi:10.1021/acs.molpharmaceut.8b00597.
51. Zhang, Z.; Lu, Z.; Yuan, Q.; Zhang, C.; Tang, Y. ROS-Responsive and active targeted drug delivery based on conjugated polymer nanoparticles for synergistic chemo-/photodynamic therapy. *J. Mater. Chem. B* **2021**, *9*, 2240-2248, doi:10.1039/d0tb02996c.
52. Xie, W.; Zhu, S.; Yang, B.; Chen, C.; Chen, S.; Liu, Y.; Nie, X.; Hao, L.; Wang, Z.; Sun, J.; et al. The Destruction of Laser-Induced Phase-Transition Nanoparticles Triggered by Low-Intensity Ultrasound: An Innovative Modality to Enhance the Immunological Treatment of Ovarian Cancer Cells. *Int. J. Nanomed.* **2019**, *14*, 9377-9393, doi:10.2147/IJN.S208404.
53. Yang, G.; Tian, J.; Chen, C.; Jiang, D.; Xue, Y.; Wang, C.; Gao, Y.; Zhang, W. An oxygen self-sufficient NIR-responsive nanosystem for enhanced PDT and chemotherapy against hypoxic tumors. *Chem. Sci.* **2019**, *10*, 5766-5772, doi:10.1039/c9sc00985j.
54. Ren, Y.; Wang, R.; Liu, Y.; Guo, H.; Zhou, X.; Yuan, X.; Liu, C.; Tian, J.; Yin, H.; Wang, Y.; et al. A hematoporphyrin-based delivery system for drug resistance reversal and tumor ablation. *Biomaterials* **2014**, *35*, 2462-2470, doi:10.1016/j.biomaterials.2013.12.004.
55. Du, C.; Liang, Y.; Ma, Q.; Sun, Q.; Qi, J.; Cao, J.; Han, S.; Liang, M.; Song, B.; Sun, Y. Intracellular tracking of drug release from pH-sensitive polymeric nanoparticles via FRET for synergistic chemo-photodynamic therapy. *J. Nanobiotechnol.* **2019**, *17*, 113, doi:10.1186/s12951-019-0547-2.
56. Pei, Q.; Hu, X.; Zheng, X.; Liu, S.; Li, Y.; Jing, X.; Xie, Z. Light-Activatable Red Blood Cell Membrane-Camouflaged Dimeric Prodrug Nanoparticles for Synergistic Photodynamic/Chemotherapy. *ACS Nano* **2018**, *12*, 1630-1641, doi:10.1021/acsnano.7b08219.
57. Chen, Y.; Gao, Y.; Li, Y.; Wang, K.; Zhu, J. Synergistic chemo-photodynamic therapy mediated by light-activated ROS-degradable nanocarriers. *J. Mater. Chem. B* **2019**, *7*, 460-468, doi:10.1039/c8tb03030h.
58. He, C.; Liu, D.; Lin, W. Self-assembled core-shell nanoparticles for combined chemotherapy and photodynamic therapy of resistant head and neck cancers. *ACS Nano* **2015**, *9*, 991-1003, doi:10.1021/nn506963h.
59. Conte, C.; Ungaro, F.; Maglio, G.; Tirino, P.; Siracusano, G.; Sciortino, M.T.; Leone, N.; Palma, G.; Barbieri, A.; Arra, C.; et al. Biodegradable core-shell nanoassemblies for the delivery of docetaxel and Zn(II)-phthalocyanine inspired by combination therapy for cancer. *J. Control. Release* **2013**, *167*, 40-52, doi:10.1016/j.jconrel.2012.12.026.
60. Gusti-Ngurah-Putu, E.P.; Huang, L.; Hsu, Y.C. Effective Combined Photodynamic Therapy with Lipid Platinum Chloride Nanoparticles Therapies of Oral Squamous Carcinoma Tumor Inhibition. *J. Clin. Med.* **2019**, *8*, 2112, doi:10.3390/jcm8122112.
61. Chang, E.; Bu, J.; Ding, L.; Lou, J.W.H.; Valic, M.S.; Cheng, M.H.Y.; Rosilio, V.; Chen, J.; Zheng, G. Porphyrin-lipid stabilized paclitaxel nanoemulsion for combined photodynamic therapy and chemotherapy. *J. Nanobiotechnol.* **2021**, *19*, 154, doi:10.1186/s12951-021-00898-1.
62. Han, Y.; An, Y.; Jia, G.; Wang, X.; He, C.; Ding, Y.; Tang, Q. Theranostic micelles based on upconversion nanoparticles for dual-modality imaging and photodynamic therapy in hepatocellular carcinoma. *Nanoscale* **2018**, *10*, 6511-6523, doi:10.1039/C7NR09717D.
63. Xing, Y.; Ding, T.; Wang, Z.; Wang, L.; Guan, H.; Tang, J.; Mo, D.; Zhang, J. Temporally Controlled Photothermal/Photodynamic and Combined Therapy for Overcoming Multidrug

Resistance of Cancer by Polydopamine Nanoclustered Micelles. *ACS Appl. Mater. Interfaces* **2019**, *11*, 13945-13953, doi:10.1021/acsami.9b00472.
64. Chen, Y.; Ren, J.; Tian, D.; Li, Y.; Jiang, H.; Zhu, J. Polymer-Upconverting Nanoparticle Hybrid Micelles for Enhanced Synergistic Chemo-Photodynamic Therapy: Effects of Emission-Absorption Spectral Match. *Biomacromolecules* **2019**, *20*, 4044-4052, doi:10.1021/acs.biomac.9b01211.
65. Wang, T.; Wang, D.; Yu, H.; Wang, M.; Liu, J.; Feng, B.; Zhou, F.; Yin, Q.; Zhang, Z.; Huang, Y.; et al. Intracellularly Acid-Switchable Multifunctional Micelles for Combinational Photo/Chemotherapy of the Drug-Resistant Tumor. *ACS Nano* **2016**, *10*, 3496-3508, doi:10.1021/acsnano.5b07706.
66. Li, F.; Liang, Y.; Wang, M.; Xu, X.; Zhao, F.; Wang, X.; Sun, Y.; Chen, W. Multifunctional nanoplatforms as cascade-responsive drug-delivery carriers for effective synergistic chemo-photodynamic cancer treatment. *J. Nanobiotechnol.* **2021**, *19*, 140, doi:10.1186/s12951-021-00876-7.
67. Tian, J.; Xiao, C.; Huang, B.; Wang, C.; Zhang, W. Janus macromolecular brushes for synergistic cascade-amplified photodynamic therapy and enhanced chemotherapy. *Acta Biomater.* **2020**, *101*, 495-506, doi:10.1016/j.actbio.2019.11.018.
68. Wang, R.; Yang, H.; Khan, A.R.; Yang, X.; Xu, J.; Ji, J.; Zhai, G. Redox-responsive hyaluronic acid-based nanoparticles for targeted photodynamic therapy/chemotherapy against breast cancer. *J. Colloid Interface Sci.* **2021**, *598*, 213-228, doi:10.1016/j.jcis.2021.04.056.
69. Xu, S.; Zhu, X.; Zhang, C.; Huang, W.; Zhou, Y.; Yan, D. Oxygen and Pt(II) self-generating conjugate for synergistic photo-chemo therapy of hypoxic tumor. *Nat. Commun.* **2018**, *9*, 2053, doi:10.1038/s41467-018-04318-1.
70. Zhu, R.; He, H.; Liu, Y.; Cao, D.; Yan, J.; Duan, S.; Chen, Y.; Yin, L. Cancer-Selective Bioreductive Chemotherapy Mediated by Dual Hypoxia-Responsive Nanomedicine upon Photodynamic Therapy-Induced Hypoxia Aggravation. *Biomacromolecules* **2019**, *20*, 2649-2656, doi:10.1021/acs.biomac.9b00428.
71. Lee, H.; Han, J.; Shin, H.; Han, H.; Na, K.; Kim, H. Combination of chemotherapy and photodynamic therapy for cancer treatment with sonoporation effects. *J. Control. Release* **2018**, *283*, 190-199, doi:10.1016/j.jconrel.2018.06.008.
72. Sun, C.Y.; Cao, Z.; Zhang, X.J.; Sun, R.; Yu, C.S.; Yang, X. Cascade-amplifying synergistic effects of chemo-photodynamic therapy using ROS-responsive polymeric nanocarriers. *Theranostics* **2018**, *8*, 2939-2953, doi:10.7150/thno.24015.
73. He, Z.; Jiang, H.; Zhang, X.; Zhang, H.; Cui, Z.; Sun, L.; Li, H.; Qian, J.; Ma, J.; Huang, J. Nano-delivery vehicle based on chlorin E6, photodynamic therapy, doxorubicin chemotherapy provides targeted treatment of HER-2 negative, alphanubeta3-positive breast cancer. *Pharmacol. Res.* **2020**, *160*, 105184, doi:10.1016/j.phrs.2020.105184.
74. Cheng, X.; He, L.; Xu, J.; Fang, Q.; Yang, L.; Xue, Y.; Wang, X.; Tang, R. Oxygen-producing catalase-based prodrug nanoparticles overcoming resistance in hypoxia-mediated chemo-photodynamic therapy. *Acta Biomater.* **2020**, *112*, 234-249, doi:10.1016/j.actbio.2020.05.035.
75. Gaio, E.; Guerrini, A.; Ballestri, M.; Varchi, G.; Ferroni, C.; Martella, E.; Columbaro, M.; Moret, F.; Reddi, E. Keratin nanoparticles co-delivering Docetaxel and Chlorin e6 promote synergic interaction between chemo- and photo-dynamic therapies. *J. Photochem. Photobiol. B* **2019**, *199*, 111598, doi:10.1016/j.jphotobiol.2019.111598.
76. Guo, Y.; Liu, H.; Xiao, H.; Yuan, M.; Liu, Y.; Sedlarik, V.; Chin, W.C.; Liu, J.; Guo, L.; Li, C. Self-assembled Camptothecin derivatives—Curcuminoids conjugate for combinatorial chemo-photodynamic therapy to enhance anti-tumor efficacy. *J. Photochem. Photobiol. B* **2021**, *215*, 112124, doi:10.1016/j.jphotobiol.2021.112124.

77. Zhang, C.; Shi, G.; Zhang, J.; Niu, J.; Huang, P.; Wang, Z.; Wang, Y.; Wang, W.; Li, C.; Kong, D. Redox- and light-responsive alginate nanoparticles as effective drug carriers for combinational anticancer therapy. *Nanoscale* **2017**, *9*, 3304-3314, doi:10.1039/c7nr00005g.
78. Kim, Y.; Uthaman, S.; Pillarisetti, S.; Noh, K.; Huh, K.M.; Park, I.K. Bioactivatable reactive oxygen species-sensitive nanoparticulate system for chemo-photodynamic therapy. *Acta Biomater.* **2020**, *108*, 273-284, doi:10.1016/j.actbio.2020.03.027.
79. Pellosi, D.S.; Paula, L.B.; de Melo, M.T.; Tedesco, A.C. Targeted and Synergic Glioblastoma Treatment: Multifunctional Nanoparticles Delivering Verteporfin as Adjuvant Therapy for Temozolomide Chemotherapy. *Mol. Pharm.* **2019**, *16*, 1009-1024, doi:10.1021/acs.molpharmaceut.8b01001.
80. Chang, J.E.; Cho, H.J.; Yi, E.; Kim, D.D.; Jheon, S. Hypocrellin B and paclitaxel-encapsulated hyaluronic acid-ceramide nanoparticles for targeted photodynamic therapy in lung cancer. *J. Photochem. Photobiol. B* **2016**, *158*, 113-121, doi:10.1016/j.jphotobiol.2016.02.035.
81. Luo, C.; Sun, B.; Wang, C.; Zhang, X.; Chen, Y.; Chen, Q.; Yu, H.; Zhao, H.; Sun, M.; Li, Z.; et al. Self-facilitated ROS-responsive nanoassembly of heterotypic dimer for synergistic chemo-photodynamic therapy. *J. Control. Release* **2019**, *302*, 79-89, doi:10.1016/j.jconrel.2019.04.001.
82. Yao, H.; Zhang, S.; Guo, X.; Li, Y.; Ren, J.; Zhou, H.; Du, B.; Zhou, J. A traceable nanoplatform for enhanced chemo-photodynamic therapy by reducing oxygen consumption. *Nanomedicine* **2019**, *20*, 101978, doi:10.1016/j.nano.2019.03.001.
83. Chen, Q.; Ma, Y.; Bai, P.; Li, Q.; Canup, B.S.B.; Long, D.; Ke, B.; Dai, F.; Xiao, B.; Li, C. Tumor Microenvironment-Responsive Nanococktails for Synergistic Enhancement of Cancer Treatment via Cascade Reactions. *ACS Appl. Mater. Interfaces* **2021**, *13*, 4861-4873, doi:10.1021/acsami.0c20268.
84. Wang, Y.; Xie, D.; Pan, J.; Xia, C.; Fan, L.; Pu, Y.; Zhang, Q.; Ni, Y.H.; Wang, J.; Hu, Q. A near infrared light-triggered human serum albumin drug delivery system with coordination bonding of indocyanine green and cisplatin for targeting photochemistry therapy against oral squamous cell cancer. *Biomater. Sci.* **2019**, *7*, 5270-5282, doi:10.1039/c9bm01192g.
85. Dag, A.; Cakilkaya, E.; Omurtag Ozgen, P.S.; Atasoy, S.; Yigit Erdem, G.; Cetin, B.; Cavus Kokuroglu, A.; Gurek, A.G. Phthalocyanine-Conjugated Glyconanoparticles for Chemo-photodynamic Combination Therapy. *Biomacromolecules* **2021**, *22*, 1555-1567, doi:10.1021/acs.biomac.0c01811.
86. Cui, D.; Huang, J.; Zhen, X.; Li, J.; Jiang, Y.; Pu, K. A Semiconducting Polymer Nano-Prodrug for Hypoxia-Activated Photodynamic Cancer Therapy. *Angew. Chem. Int. Ed. Engl.* **2019**, *58*, 5920-5924, doi:10.1002/anie.201814730.
87. Zong, J.; Peng, H.; Qing, X.; Fan, Z.; Xu, W.; Du, X.; Shi, R.; Zhang, Y. pH-Responsive Pluronic F127-Lenvatinib-Encapsulated Halogenated Boron-Dipyrromethene Nanoparticles for Combined Photodynamic Therapy and Chemotherapy of Liver Cancer. *ACS Omega* **2021**, *6*, 12331-12342, doi:10.1021/acsomega.1c01346.
88. Wang, Q.; Zhang, X.; Sun, Y.; Wang, L.; Ding, L.; Zhu, W.H.; Di, W.; Duan, Y.R. Gold-caged copolymer nanoparticles as multimodal synergistic photodynamic/photothermal/chemotherapy platform against lethality androgen-resistant prostate cancer. *Biomaterials* **2019**, *212*, 73-86, doi:10.1016/j.biomaterials.2019.05.009.
89. Yao, C.; Wang, W.; Wang, P.; Zhao, M.; Li, X.; Zhang, F. Near-Infrared Upconversion Mesoporous Cerium Oxide Hollow Biophotocatalyst for Concurrent pH-/H2 O2-Responsive O2-Evolving Synergetic Cancer Therapy. *Adv. Mater.* **2018**, *30*, 1704833, doi:10.1002/adma.201704833.
90. Guo, Z.; Zheng, K.; Tan, Z.; Liu, Y.; Zhao, Z.; Zhu, G.; Ma, K.; Cui, C.; Wang, L.; Kang, T. Overcoming drug resistance with functional mesoporous titanium dioxide nanoparticles

combining targeting, drug delivery and photodynamic therapy. *J. Mater. Chem. B* **2018**, *6*, 7750-7759, doi:10.1039/c8tb01810c.
91. Zhang, X.; Huang, B.; Shen, Y.; Yang, C.; Huang, Z.; Huang, Y.; Xu, X.; Jiang, Y.; Sun, X.; Li, X.; et al. Near infrared light triggered reactive oxygen species responsive nanoparticles for chemo-photodynamic combined therapy. *J. Mater. Chem. B* **2018**, *6*, 2347-2357, doi:10.1039/c8tb00308d.
92. Montaseri, H.; Kruger, C.A.; Abrahamse, H. Inorganic Nanoparticles Applied for Active Targeted Photodynamic Therapy of Breast Cancer. *Pharmaceutics* **2021**, *13*, 296, doi:10.3390/pharmaceutics13030296.
93. Zhang, T.; Liu, H.; Li, L.; Guo, Z.; Song, J.; Yang, X.; Wan, G.; Li, R.; Wang, Y. Leukocyte/platelet hybrid membrane-camouflaged dendritic large pore mesoporous silica nanoparticles co-loaded with photo/chemotherapeutic agents for triple negative breast cancer combination treatment. *Bioact. Mater.* **2021**, *6*, 3865-3878, doi:10.1016/j.bioactmat.2021.04.004.
94. Bi, H.; Dai, Y.; Yang, P.; Xu, J.; Yang, D.; Gai, S.; He, F.; Liu, B.; Zhong, C.; An, G.; et al. Glutathione Mediated Size-Tunable UCNPs-Pt(IV)-ZnFe2 O4 Nanocomposite for Multiple Bioimaging Guided Synergetic Therapy. *Small* **2018**, *14*, e1703809, doi:10.1002/smll.201703809.
95. Dong, S.; Xu, J.; Jia, T.; Xu, M.; Zhong, C.; Yang, G.; Li, J.; Yang, D.; He, F.; Gai, S.; et al. Upconversion-mediated ZnFe2O4 nanoplatform for NIR-enhanced chemodynamic and photodynamic therapy. *Chem. Sci.* **2019**, *10*, 4259-4271, doi:10.1039/c9sc00387h.
96. Hou, B.; Yang, W.; Dong, C.; Zheng, B.; Zhang, Y.; Wu, J.; Wang, H.; Chang, J. Controlled co-release of doxorubicin and reactive oxygen species for synergistic therapy by NIR remote-triggered nanoimpellers. *Mater. Sci. Eng. C Mater. Biol. Appl.* **2017**, *74*, 94-102, doi:10.1016/j.msec.2017.02.016.
97. Ai, F.; Sun, T.; Xu, Z.; Wang, Z.; Kong, W.; To, M.W.; Wang, F.; Zhu, G. An upconversion nanoplatform for simultaneous photodynamic therapy and Pt chemotherapy to combat cisplatin resistance. *Dalton Trans.* **2016**, *45*, 13052-13060, doi:10.1039/c6dt01404f.
98. Jin, F.; Qi, J.; Liu, D.; You, Y.; Shu, G.; Du, Y.; Wang, J.; Xu, X.; Ying, X.; Ji, J.; et al. Cancer-cell-biomimetic Upconversion nanoparticles combining chemo-photodynamic therapy and CD73 blockade for metastatic triple-negative breast cancer. *J. Control. Release* **2021**, *337*, 90-104, doi:10.1016/j.jconrel.2021.07.021.
99. Zhou, F.; Zheng, B.; Zhang, Y.; Wu, Y.; Wang, H.; Chang, J. Construction of near-infrared light-triggered reactive oxygen species-sensitive (UCN/SiO2-RB + DOX)@PPADT nanoparticles for simultaneous chemotherapy and photodynamic therapy. *Nanotechnology* **2016**, *27*, 235601, doi:10.1088/0957-4484/27/23/235601.
100. Liu, G.; Jiang, F.; Chen, Y.; Yu, C.; Ding, B.; Shao, S.; Jia, M.; Ma, P.; Fu, Z.; Lin, J. Superior temperature sensing of small-sized upconversion nanocrystals for simultaneous bioimaging and enhanced synergetic therapy. *Nanomedicine* **2020**, *24*, 102135, doi:10.1016/j.nano.2019.102135.
101. Panikar, S.S.; Ramirez-Garcia, G.; Vallejo-Cardona, A.A.; Banu, N.; Patron-Soberano, O.A.; Cialla-May, D.; Camacho-Villegas, T.A.; de la Rosa, E. Novel anti-HER2 peptide-conjugated theranostic nanoliposomes combining NaYF4:Yb,Er nanoparticles for NIR-activated bioimaging and chemo-photodynamic therapy against breast cancer. *Nanoscale* **2019**, *11*, 20598-20613, doi:10.1039/c9nr06535k.
102. Dong, C.; Liu, Z.; Wang, S.; Zheng, B.; Guo, W.; Yang, W.; Gong, X.; Wu, X.; Wang, H.; Chang, J. A Protein-Polymer Bioconjugate-Coated Upconversion Nanosystem for Simultaneous Tumor Cell Imaging, Photodynamic Therapy, and Chemotherapy. *ACS Appl. Mater. Interfaces* **2016**, *8*, 32688-32698, doi:10.1021/acsami.6b11803.

103. Tian, G.; Ren, W.; Yan, L.; Jian, S.; Gu, Z.; Zhou, L.; Jin, S.; Yin, W.; Li, S.; Zhao, Y. Red-emitting upconverting nanoparticles for photodynamic therapy in cancer cells under near-infrared excitation. *Small* **2013**, *9*, 1929-1938, doi:10.1002/smll.201201437.
104. Ji, Y.; Lu, F.; Hu, W.; Zhao, H.; Tang, Y.; Li, B.; Hu, X.; Li, X.; Lu, X.; Fan, Q.; et al. Tandem activated photodynamic and chemotherapy: Using pH-Sensitive nanosystems to realize different tumour distributions of photosensitizer/prodrug for amplified combination therapy. *Biomaterials* **2019**, *219*, 119393, doi:10.1016/j.biomaterials.2019.119393.
105. Gulzar, A.; Xu, J.; Xu, L.; Yang, P.; He, F.; Yang, D.; An, G.; Ansari, M.B. Redox-responsive UCNPs-DPA conjugated NGO-PEG-BPEI-DOX for imaging-guided PTT and chemotherapy for cancer treatment. *Dalton Trans.* **2018**, *47*, 3921-3930, doi:10.1039/c7dt04093h.
106. Jin, F.; Qi, J.; Zhu, M.; Liu, D.; You, Y.; Shu, G.; Du, Y.; Wang, J.; Yu, H.; Sun, M.; et al. NIR-Triggered Sequentially Responsive Nanocarriers Amplified Cascade Synergistic Effect of Chemo-Photodynamic Therapy with Inspired Antitumor Immunity. *ACS Appl. Mater. Interfaces* **2020**, *12*, 32372-32387, doi:10.1021/acsami.0c07503.
107. Zhang, W.; Shen, J.; Su, H.; Mu, G.; Sun, J.H.; Tan, C.P.; Liang, X.J.; Ji, L.N.; Mao, Z.W. Co-Delivery of Cisplatin Prodrug and Chlorin e6 by Mesoporous Silica Nanoparticles for Chemo-Photodynamic Combination Therapy to Combat Drug Resistance. *ACS Appl. Mater. Interfaces* **2016**, *8*, 13332-13340, doi:10.1021/acsami.6b03881.
108. Su, J.; Sun, H.; Meng, Q.; Zhang, P.; Yin, Q.; Li, Y. Enhanced Blood Suspensibility and Laser-Activated Tumor-specific Drug Release of Theranostic Mesoporous Silica Nanoparticles by Functionalizing with Erythrocyte Membranes. *Theranostics* **2017**, *7*, 523-537, doi:10.7150/thno.17259.
109. Li, S.; Zhang, Y.; He, X.W.; Li, W.Y.; Zhang, Y.K. Multifunctional mesoporous silica nanoplatform based on silicon nanoparticles for targeted two-photon-excited fluorescence imaging-guided chemo/photodynamic synergetic therapy in vitro. *Talanta* **2020**, *209*, 120552, doi:10.1016/j.talanta.2019.120552.
110. Wang, H.; Zhang, C.; Zhang, Y.; Tian, R.; Cheng, G.; Pan, H.; Cui, M.; Chang, J. An efficient delivery of photosensitizers and hypoxic prodrugs for a tumor combination therapy by membrane camouflage nanoparticles. *J. Mater. Chem. B* **2020**, *8*, 2876-2886, doi:10.1039/d0tb00235f.
111. Zhang, P.J.; Liu, M.D.; Fan, F.Y.; Liu, K.X. A Study on Mesoporous Silica Loaded with Novel Photosensitizers HCE6 and Oxaliplatin for the Treatment of Cholangiocarcinoma. *Front. Oncol.* **2021**, *11*, 665182, doi:10.3389/fonc.2021.665182.
112. Wen, J.; Yang, K.; Ding, X.; Li, H.; Xu, Y.; Liu, F.; Sun, S. In Situ Formation of Homogeneous Tellurium Nanodots in Paclitaxel-Loaded MgAl Layered Double Hydroxide Gated Mesoporous Silica Nanoparticles for Synergistic Chemo/PDT/PTT Trimode Combinatorial Therapy. *Inorg. Chem.* **2019**, *58*, 2987-2996, doi:10.1021/acs.inorgchem.8b02821.
113. Cheng, D.; Ji, Y.; Wang, B.; Jin, T.; Xu, Y.; Qian, X.; Zhu, W. Enzyme/GSH dual-responsive biodegradable nanohybrid for spatiotemporally specific photodynamic and hypoxia-augmented therapy against tumors. *Int. J. Pharm.* **2021**, *603*, 120730, doi:10.1016/j.ijpharm.2021.120730.
114. Wen, J.; Yang, K.; Xu, Y.; Li, H.; Liu, F.; Sun, S. Construction of A Triple-Stimuli-Responsive System Based on Cerium Oxide Coated Mesoporous Silica Nanoparticles. *Sci. Rep.* **2016**, *6*, 38931, doi:10.1038/srep38931.
115. Zou, R.; Gao, Y.; Zhang, Y.; Jiao, J.; Wong, K.L.; Wang, J. (68)Ga-Labeled Magnetic-NIR Persistent Luminescent Hybrid Mesoporous Nanoparticles for Multimodal Imaging-Guided Chemotherapy and Photodynamic Therapy. *ACS Appl. Mater. Interfaces* **2021**, *13*, 9667-9680, doi:10.1021/acsami.0c21623.

116. Zheng, T.; Wang, W.; Wu, F.; Zhang, M.; Shen, J.; Sun, Y. Zwitterionic Polymer-Gated Au@TiO_2 Core-Shell Nanoparticles for Imaging-Guided Combined Cancer Therapy. *Theranostics* **2019**, *9*, 5035-5048, doi:10.7150/thno.35418.
117. Feng, Q.; Zhang, Y.; Zhang, W.; Hao, Y.; Wang, Y.; Zhang, H.; Hou, L.; Zhang, Z. Programmed near-infrared light-responsive drug delivery system for combined magnetic tumor-targeting magnetic resonance imaging and chemo-phototherapy. *Acta Biomater.* **2017**, *49*, 402-413, doi:10.1016/j.actbio.2016.11.035.
118. Liu, B.; Li, C.; Chen, G.; Liu, B.; Deng, X.; Wei, Y.; Xia, J.; Xing, B.; Ma, P.; Lin, J. Synthesis and Optimization of MoS2@Fe3O4-ICG/Pt(IV) Nanoflowers for MR/IR/PA Bioimaging and Combined PTT/PDT/Chemotherapy Triggered by 808 nm Laser. *Adv. Sci.* **2017**, *4*, 1600540, doi:10.1002/advs.201600540.
119. Fan, S.; Zhang, Y.; Tan, H.; Xue, C.; He, Y.; Wei, X.; Zha, Y.; Niu, J.; Liu, Y.; Cheng, Y.; et al. Manganese/iron-based nanoprobes for photodynamic/chemotherapy combination therapy of tumor guided by multimodal imaging. *Nanoscale* **2021**, *13*, 5383-5399, doi:10.1039/d0nr08831e.
120. Yang, R.; Hou, M.; Gao, Y.; Lu, S.; Zhang, L.; Xu, Z.; Li, C.M.; Kang, Y.; Xue, P. Biomineralization-Inspired Crystallization of Manganese Oxide on Silk Fibroin Nanoparticles for In Vivo MR/Fluorescence Imaging-Assisted Tri-Modal Therapy of Cancer. *Theranostics* **2019**, *9*, 6314-6333, doi:10.7150/thno.36252.
121. Huang, X.; Wu, J.; He, M.; Hou, X.; Wang, Y.; Cai, X.; Xin, H.; Gao, F.; Chen, Y. Combined Cancer Chemo-Photodynamic and Photothermal Therapy Based on ICG/PDA/TPZ-Loaded Nanoparticles. *Mol. Pharm.* **2019**, *16*, 2172-2183, doi:10.1021/acs.molpharmaceut.9b00119.
122. Zhao, Q.G.; Wang, J.; Zhang, Y.P.; Zhang, J.; Tang, A.N.; Kong, D.M. A ZnO-gated porphyrinic metal-organic framework-based drug delivery system for targeted bimodal cancer therapy. *J. Mater. Chem. B* **2018**, *6*, 7898-7907, doi:10.1039/c8tb02663g.
123. Cui, L.; Lin, Q.; Jin, C.S.; Jiang, W.; Huang, H.; Ding, L.; Muhanna, N.; Irish, J.C.; Wang, F.; Chen, J.; et al. A PEGylation-Free Biomimetic Porphyrin Nanoplatform for Personalized Cancer Theranostics. *ACS Nano* **2015**, *9*, 4484-4495, doi:10.1021/acsnano.5b01077.
124. He, Z.; Dai, Y.; Li, X.; Guo, D.; Liu, Y.; Huang, X.; Jiang, J.; Wang, S.; Zhu, G.; Zhang, F.; et al. Hybrid Nanomedicine Fabricated from Photosensitizer-Terminated Metal-Organic Framework Nanoparticles for Photodynamic Therapy and Hypoxia-Activated Cascade Chemotherapy. *Small* **2019**, *15*, e1804131, doi:10.1002/smll.201804131.
125. Han, L.; Wang, Y.; Huang, X.; Liu, F.; Ma, C.; Feng, F.; Zhang, J.; Liu, W.; Qu, W.; Pang, H.; et al. Specific-oxygen-supply functionalized core-shell nanoparticles for smart mutual-promotion between photodynamic therapy and gambogic acid-induced chemotherapy. *Biomaterials* **2020**, *257*, 120228, doi:10.1016/j.biomaterials.2020.120228.
126. Fang, C.; Cen, D.; Wang, Y.; Wu, Y.; Cai, X.; Li, X.; Han, G. ZnS@ZIF-8 core-shell nanoparticles incorporated with ICG and TPZ to enable H2S-amplified synergistic therapy. *Theranostics* **2020**, *10*, 7671-7682, doi:10.7150/thno.45079.
127. Yu, G.; Zhu, B.; Shao, L.; Zhou, J.; Saha, M.L.; Shi, B.; Zhang, Z.; Hong, T.; Li, S.; Chen, X.; et al. Host-guest complexation-mediated codelivery of anticancer drug and photosensitizer for cancer photochemotherapy. *Proc. Natl. Acad. Sci. USA* **2019**, *116*, 6618-6623, doi:10.1073/pnas.1902029116.
128. Yang, B.; Liu, H.; Yang, H.; Chen, W.; Wu, J.; Feng, X.; Tong, R.; Yu, H.; Chen, Y.; Lv, Z.; et al. Combinatorial photochemotherapy on liver cancer stem cells with organoplatinum(ii) metallacage-based nanoparticles. *J. Mater. Chem. B* **2019**, *7*, 6476-6487, doi:10.1039/c9tb01299k.
129. Yang, R.; Hou, M.; Gao, Y.; Zhang, L.; Xu, Z.; Kang, Y.; Xue, P. Indocyanine green-modified hollow mesoporous Prussian blue nanoparticles loading doxorubicin for fluorescence-guided tri-modal combination therapy of cancer. *Nanoscale* **2019**, *11*, 5717-5731, doi:10.1039/c8nr10430a.

130. Li, M.; Wang, Y.; Lin, H.; Qu, F. Hollow CuS nanocube as nanocarrier for synergetic chemo/photothermal/photodynamic therapy. *Mater. Sci. Eng. C Mater. Biol. Appl.* **2019**, *96*, 591-598, doi:10.1016/j.msec.2018.11.020.
131. Srinivasan, S.; Bhardwaj, V.; Nagasetti, A.; Fernandez-Fernandez, A.; McGoron, A.J. Multifunctional Surface-Enhanced Raman Spectroscopy-Detectable Silver Nanoparticles Combined Photodynamic Therapy and pH-Triggered Chemotherapy. *J. Biomed. Nanotechnol.* **2016**, *12*, 2202-2219, doi:10.1166/jbn.2016.2312.
132. Gu, Z.; Da Silva, C.G.; Van der Maaden, K.; Ossendorp, F.; Cruz, L.J. Liposome-Based Drug Delivery Systems in Cancer Immunotherapy. *Pharmaceutics* **2020**, *12*, 1054, doi:10.3390/pharmaceutics12111054.
133. Falk-Mahapatra, R.; Gollnick, S.O. Photodynamic Therapy and Immunity: An Update. *Photochem. Photobiol.* **2020**, *96*, 550-559, doi:10.1111/php.13253.
134. Zeng, J.Y.; Zou, M.Z.; Zhang, M.; Wang, X.S.; Zeng, X.; Cong, H.; Zhang, X.Z. pi-Extended Benzoporphyrin-Based Metal-Organic Framework for Inhibition of Tumor Metastasis. *ACS Nano* **2018**, *12*, 4630-4640, doi:10.1021/acsnano.8b01186.
135. Ni, J.; Song, J.; Wang, B.; Hua, H.; Zhu, H.; Guo, X.; Xiong, S.; Zhao, Y. Dendritic cell vaccine for the effective immunotherapy of breast cancer. *Biomed. Pharmacother.* **2020**, *126*, 110046, doi:10.1016/j.biopha.2020.110046.
136. Dai, W.; Lu, S.; Zeng, W.; Lee, D. Lipid Coated and Chlorin e6 Loaded Calcium Carbonate for Effective In Situ Immunotheraphy of Colorectal Cancer. *J. Biomed. Nanotechnol.* **2020**, *16*, 1196-1204, doi:10.1166/jbn.2020.2965.
137. Fang, L.; Zhao, Z.; Wang, J.; Zhang, P.; Ding, Y.; Jiang, Y.; Wang, D.; Li, Y. Engineering autologous tumor cell vaccine to locally mobilize antitumor immunity in tumor surgical bed. *Sci. Adv.* **2020**, *6*, eaba4024, doi:10.1126/sciadv.aba4024.
138. Xu, C.; Nam, J.; Hong, H.; Xu, Y.; Moon, J.J. Positron Emission Tomography-Guided Photodynamic Therapy with Biodegradable Mesoporous Silica Nanoparticles for Personalized Cancer Immunotherapy. *ACS Nano* **2019**, *13*, 12148-12161, doi:10.1021/acsnano.9b06691.
139. Yan, S.; Zeng, X.; Tang, Y.; Liu, B.F.; Wang, Y.; Liu, X. Activating Antitumor Immunity and Antimetastatic Effect through Polydopamine-Encapsulated Core-Shell Upconversion Nanoparticles. *Adv. Mater.* **2019**, *31*, e1905825, doi:10.1002/adma.201905825.
140. Xu, J.; Xu, L.; Wang, C.; Yang, R.; Zhuang, Q.; Han, X.; Dong, Z.; Zhu, W.; Peng, R.; Liu, Z. Near-Infrared-Triggered Photodynamic Therapy with Multitasking Upconversion Nanoparticles in Combination with Checkpoint Blockade for Immunotherapy of Colorectal Cancer. *ACS Nano* **2017**, *11*, 4463-4474, doi:10.1021/acsnano.7b00715.
141. Wang, Z.; Zhang, F.; Shao, D.; Chang, Z.; Wang, L.; Hu, H.; Zheng, X.; Li, X.; Chen, F.; Tu, Z.; et al. Janus Nanobullets Combine Photodynamic Therapy and Magnetic Hyperthermia to Potentiate Synergetic Anti-Metastatic Immunotherapy. *Adv. Sci.* **2019**, *6*, 1901690, doi:10.1002/advs.201901690.
142. Meng, Z.; Zhou, X.; Xu, J.; Han, X.; Dong, Z.; Wang, H.; Zhang, Y.; She, J.; Xu, L.; Wang, C.; et al. Light-Triggered In Situ Gelation to Enable Robust Photodynamic-Immunotherapy by Repeated Stimulations. *Adv. Mater.* **2019**, *31*, e1900927, doi:10.1002/adma.201900927.
143. Yang, G.; Xu, L.; Chao, Y.; Xu, J.; Sun, X.; Wu, Y.; Peng, R.; Liu, Z. Hollow MnO2 as a tumor-microenvironment-responsive biodegradable nano-platform for combination therapy favoring antitumor immune responses. *Nat. Commun.* **2017**, *8*, 902, doi:10.1038/s41467-017-01050-0.
144. Liu, H.; Hu, Y.; Sun, Y.; Wan, C.; Zhang, Z.; Dai, X.; Lin, Z.; He, Q.; Yang, Z.; Huang, P.; et al. Co-Delivery of Bee Venom Melittin and a Photosensitizer with an Organic-Inorganic Hybrid

Nanocarrier for Photodynamic Therapy and Immunotherapy. *ACS Nano* **2019**, *13*, 12638-12652, doi:10.1021/acsnano.9b04181.
145. Hu, L.; Cao, Z.; Ma, L.; Liu, Z.; Liao, G.; Wang, J.; Shen, S.; Li, D.; Yang, X. The potentiated checkpoint blockade immunotherapy by ROS-responsive nanocarrier-mediated cascade chemo-photodynamic therapy. *Biomaterials* **2019**, *223*, 119469, doi:10.1016/j.biomaterials.2019.119469.
146. Zhang, M.; Wang, W.; Wu, F.; Zheng, T.; Ashley, J.; Mohammadniaei, M.; Zhang, Q.; Wang, M.; Li, L.; Shen, J.; et al. Biodegradable Poly(gamma-glutamic acid)@glucose oxidase@carbon dot nanoparticles for simultaneous multimodal imaging and synergetic cancer therapy. *Biomaterials* **2020**, *252*, 120106, doi:10.1016/j.biomaterials.2020.120106.
147. Yang, W.; Zhu, G.; Wang, S.; Yu, G.; Yang, Z.; Lin, L.; Zhou, Z.; Liu, Y.; Dai, Y.; Zhang, F.; et al. In Situ Dendritic Cell Vaccine for Effective Cancer Immunotherapy. *ACS Nano* **2019**, *13*, 3083-3094, doi:10.1021/acsnano.8b08346.
148. Yu, X.; Gao, D.; Gao, L.; Lai, J.; Zhang, C.; Zhao, Y.; Zhong, L.; Jia, B.; Wang, F.; Chen, X.; et al. Inhibiting Metastasis and Preventing Tumor Relapse by Triggering Host Immunity with Tumor-Targeted Photodynamic Therapy Using Photosensitizer-Loaded Functional Nanographenes. *ACS Nano* **2017**, *11*, 10147-10158, doi:10.1021/acsnano.7b04736.
149. Cai, Z.; Xin, F.; Wei, Z.; Wu, M.; Lin, X.; Du, X.; Chen, G.; Zhang, D.; Zhang, Z.; Liu, X.; et al. Photodynamic Therapy Combined with Antihypoxic Signaling and CpG Adjuvant as an In Situ Tumor Vaccine Based on Metal-Organic Framework Nanoparticles to Boost Cancer Immunotherapy. *Adv. Healthc. Mater.* **2020**, *9*, e1900996, doi:10.1002/adhm.201900996.
150. Liu, Y.; Pan, Y.; Cao, W.; Xia, F.; Liu, B.; Niu, J.; Alfranca, G.; Sun, X.; Ma, L.; de la Fuente, J.M.; et al. A tumor microenvironment responsive biodegradable CaCO3/MnO2-based nanoplatform for the enhanced photodynamic therapy and improved PD-L1 immunotherapy. *Theranostics* **2019**, *9*, 6867-6884, doi:10.7150/thno.37586.
151. Chen, Q.; Xu, L.; Liang, C.; Wang, C.; Peng, R.; Liu, Z. Photothermal therapy with immune-adjuvant nanoparticles together with checkpoint blockade for effective cancer immunotherapy. *Nat. Commun.* **2016**, *7*, 13193, doi:10.1038/ncomms13193.
152. Li, Y.; Du, Y.; Liang, X.; Sun, T.; Xue, H.; Tian, J.; Jin, Z. EGFR-targeted liposomal nanohybrid cerasomes: Theranostic function and immune checkpoint inhibition in a mouse model of colorectal cancer. *Nanoscale* **2018**, *10*, 16738-16749, doi:10.1039/c8nr05803b.
153. Zhou, L.; Chen, L.; Hu, X.; Lu, Y.; Liu, W.; Sun, Y.; Yao, T.; Dong, C.; Shi, S. A Cu9S5 nanoparticle-based CpG delivery system for synergistic photothermal-, photodynamic- and immunotherapy. *Commun. Biol.* **2020**, *3*, 343, doi:10.1038/s42003-020-1070-6.
154. He, C.; Duan, X.; Guo, N.; Chan, C.; Poon, C.; Weichselbaum, R.R.; Lin, W. Core-shell nanoscale coordination polymers combine chemotherapy and photodynamic therapy to potentiate checkpoint blockade cancer immunotherapy. *Nat. Commun.* **2016**, *7*, 12499, doi:10.1038/ncomms12499.
155. Duan, X.; Chan, C.; Guo, N.; Han, W.; Weichselbaum, R.R.; Lin, W. Photodynamic Therapy Mediated by Nontoxic Core-Shell Nanoparticles Synergizes with Immune Checkpoint Blockade to Elicit Antitumor Immunity and Antimetastatic Effect on Breast Cancer. *J. Am. Chem. Soc.* **2016**, *138*, 16686-16695, doi:10.1021/jacs.6b09538.
156. Marrache, S.; Choi, J.H.; Tundup, S.; Zaver, D.; Harn, D.A.; Dhar, S. Immune stimulating photoactive hybrid nanoparticles for metastatic breast cancer. *Integr. Biol.* **2013**, *5*, 215-223, doi:10.1039/c2ib20125a.
157. Zhang, Y.; Liao, Y.; Tang, Q.; Lin, J.; Huang, P. Biomimetic Nanoemulsion for Synergistic Photodynamic-Immunotherapy Against Hypoxic Breast Tumor. *Angew. Chem. Int. Ed. Engl.* **2021**, *60*, 10647-10653, doi:10.1002/anie.202015590.

158. Hu, C.; Cai, L.; Liu, S.; Liu, Y.; Zhou, Y.; Pang, M. Copper-Doped Nanoscale Covalent Organic Polymer for Augmented Photo/Chemodynamic Synergistic Therapy and Immunotherapy. *Bioconjug. Chem.* **2020**, *31*, 1661-1670, doi:10.1021/acs.bioconjchem.0c00209.
159. Kleinovink, J.W.; van Hall, T.; Ossendorp, F.; Fransen, M.F. PD-L1 immune suppression in cancer: Tumor cells or host cells? *Oncoimmunology* **2017**, *6*, e1325982, doi:10.1080/2162402X.2017.1325982.
160. Anand, S.; Chan, T.A.; Hasan, T.; Maytin, E.V. Current Prospects for Treatment of Solid Tumors via Photodynamic, Photothermal, or Ionizing Radiation Therapies Combined with Immune Checkpoint Inhibition (A Review). *Pharmaceuticals* **2021**, *14*, 447, doi:10.3390/ph14050447.
161. Chung, C.K.; Fransen, M.F.; van der Maaden, K.; Campos, Y.; Garcia-Couce, J.; Kralisch, D.; Chan, A.; Ossendorp, F.; Cruz, L.J. Thermosensitive hydrogels as sustained drug delivery system for CTLA-4 checkpoint blocking antibodies. *J. Control. Release* **2020**, *323*, 1-11, doi:10.1016/j.jconrel.2020.03.050.
162. Nikpoor, A.R.; Tavakkol-Afshari, J.; Sadri, K.; Jalali, S.A.; Jaafari, M.R. Improved tumor accumulation and therapeutic efficacy of CTLA-4-blocking antibody using liposome-encapsulated antibody: In vitro and in vivo studies. *Nanomedicine* **2017**, *13*, 2671-2682, doi:10.1016/j.nano.2017.08.010.
163. Cazares-Cortes, E.; Cabana, S.; Boitard, C.; Nehlig, E.; Griffete, N.; Fresnais, J.; Wilhelm, C.; Abou-Hassan, A.; Menager, C. Recent insights in magnetic hyperthermia: From the "hot-spot" effect for local delivery to combined magneto-photo-thermia using magneto-plasmonic hybrids. *Adv. Drug Deliv. Rev.* **2019**, *138*, 233-246, doi:10.1016/j.addr.2018.10.016.
164. Harari, A.; Graciotti, M.; Bassani-Sternberg, M.; Kandalaft, L.E. Antitumour dendritic cell vaccination in a priming and boosting approach. *Nat. Rev. Drug Discov.* **2020**, *19*, 635-652, doi:10.1038/s41573-020-0074-8.
165. Bouzid, R.; Peppelenbosch, M.; Buschow, S.I. Opportunities for Conventional and in Situ Cancer Vaccine Strategies and Combination with Immunotherapy for Gastrointestinal Cancers, A Review. *Cancers* **2020**, *12*, 1121, doi:10.3390/cancers12051121.
166. Gollnick, S.O.; Vaughan, L.; Henderson, B.W. Generation of effective antitumor vaccines using photodynamic therapy. *Cancer Res.* **2002**, *62*, 1604-1608.
167. Turubanova, V.D.; Balalaeva, I.V.; Mishchenko, T.A.; Catanzaro, E.; Alzeibak, R.; Peskova, N.N.; Efimova, I.; Bachert, C.; Mitroshina, E.V.; Krysko, O.; et al. Immunogenic cell death induced by a new photodynamic therapy based on photosens and photodithazine. *J. Immunother. Cancer* **2019**, *7*, 350, doi:10.1186/s40425-019-0826-3.
168. Korbelik, M.; Banath, J.; Zhang, W. Mreg Activity in Tumor Response to Photodynamic Therapy and Photodynamic Therapy-Generated Cancer Vaccines. *Cancers* **2016**, *8*, 94, doi:10.3390/cancers8100094.
169. Korbelik, M.; Banath, J.; Saw, K.M. Immunoregulatory Cell Depletion Improves the Efficacy of Photodynamic Therapy-Generated Cancer Vaccines. *Int. J. Mol. Sci.* **2015**, *16*, 27005-27014, doi:10.3390/ijms161126008.
170. Ji, J.; Fan, Z.; Zhou, F.; Wang, X.; Shi, L.; Zhang, H.; Wang, P.; Yang, D.; Zhang, L.; Chen, W.R.; et al. Improvement of DC vaccine with ALA-PDT induced immunogenic apoptotic cells for skin squamous cell carcinoma. *Oncotarget* **2015**, *6*, 17135-17146, doi:10.18632/oncotarget.3529.
171. Hwang, H.S.; Cherukula, K.; Bang, Y.J.; Vijayan, V.; Moon, M.J.; Thiruppathi, J.; Puth, S.; Jeong, Y.Y.; Park, I.K.; Lee, S.E.; et al. Combination of Photodynamic Therapy and a Flagellin-Adjuvanted Cancer Vaccine Potentiated the Anti-PD-1-Mediated Melanoma Suppression. *Cells* **2020**, *9*, 2432, doi:10.3390/cells9112432.
172. Kleinovink, J.W.; van Driel, P.B.; Snoeks, T.J.; Prokopi, N.; Fransen, M.F.; Cruz, L.J.; Mezzanotte, L.; Chan, A.; Lowik, C.W.; Ossendorp, F. Combination of Photodynamic Therapy

and Specific Immunotherapy Efficiently Eradicates Established Tumors. *Clin. Cancer Res.* **2016**, *22*, 1459-1468, doi:10.1158/1078-0432.CCR-15-0515.
173. Trempolec, N.; Doix, B.; Degavre, C.; Brusa, D.; Bouzin, C.; Riant, O.; Feron, O. Photodynamic Therapy-Based Dendritic Cell Vaccination Suited to Treat Peritoneal Mesothelioma. *Cancers* **2020**, *12*, 545, doi:10.3390/cancers12030545.
174. Khaled, Y.S.; Wright, K.; Melcher, A.; Jayne, D. Anti-cancer effects of oncolytic viral therapy combined with photodynamic therapy in human pancreatic cancer cell lines. *Lancet* **2015**, *385* (Suppl. S1), S56, doi:10.1016/S0140-6736(15)60371-3.
175. Alzeibak, R.; Mishchenko, T.A.; Shilyagina, N.Y.; Balalaeva, I.V.; Vedunova, M.V.; Krysko, D.V. Targeting immunogenic cancer cell death by photodynamic therapy: Past, present and future. *J. Immunother. Cancer.* **2021**, *9*, e001926, doi:10.1136/jitc-2020-001926.
176. Leroux-Roels, G. Unmet needs in modern vaccinology: Adjuvants to improve the immune response. *Vaccine* **2010**, *28* (Suppl. S3), C25-C36, doi:10.1016/j.vaccine.2010.07.021.
177. Vasilakos, J.P.; Tomai, M.A. The use of Toll-like receptor 7/8 agonists as vaccine adjuvants. *Expert Rev. Vaccines* **2013**, *12*, 809-819, doi:10.1586/14760584.2013.811208.
178. Huis in 't Veld, R.V.; Da Silva, C.G.; Jager, M.J.; Cruz, L.J.; Ossendorp, F. Combining Photodynamic Therapy with Immunostimulatory Nanoparticles Elicits Effective Anti-Tumor Immune Responses in Preclinical Murine Models. *Pharmaceutics* **2021**, *13*, 1470, doi:10.3390/pharmaceutics13091470.
179. Huis In 't Veld, R.V.; Ritsma, L.; Kleinovink, J.W.; Que, I.; Ossendorp, F.; Cruz, L.J. Photodynamic cancer therapy enhances accumulation of nanoparticles in tumor-associated myeloid cells. *J. Control. Release* **2020**, *320*, 19-31, doi:10.1016/j.jconrel.2019.12.052.
180. Chen, W.R.; Korbelik, M.; Bartels, K.E.; Liu, H.; Sun, J.; Nordquist, R.E. Enhancement of laser cancer treatment by a chitosan-derived immunoadjuvant. *Photochem. Photobiol.* **2005**, *81*, 190-195, doi:10.1562/2004-07-20-RA-236.
181. Bode, C.; Zhao, G.; Steinhagen, F.; Kinjo, T.; Klinman, D.M. CpG DNA as a vaccine adjuvant. *Expert Rev. Vaccines* **2011**, *10*, 499-511, doi:10.1586/erv.10.174.
182. Soler, D.C.; Ohtola, J.; Sugiyama, H.; Rodriguez, M.E.; Han, L.; Oleinick, N.L.; Lam, M.; Baron, E.D.; Cooper, K.D.; McCormick, T.S. Activated T cells exhibit increased uptake of silicon phthalocyanine Pc 4 and increased susceptibility to Pc 4-photodynamic therapy-mediated cell death. *Photochem. Photobiol. Sci.* **2016**, *15*, 822-831, doi:10.1039/c6pp00058d.
183. Li, L.; Yang, Z.; Fan, W.; He, L.; Cui, C.; Zou, J.; Tang, W.; Jacobson, O.; Wang, Z.; Niu, G.; et al. In Situ Polymerized Hollow Mesoporous Organosilica Biocatalysis Nanoreactor for Enhancing ROS-Mediated Anticancer Therapy. *Adv. Funct. Mater.* **2020**, *30*, 1907716, doi:10.1002/adfm.201907716.
184. Korbelik, M.; Naraparaju, V.R.; Yamamoto, N. Macrophage-directed immunotherapy as adjuvant to photodynamic therapy of cancer. *Br. J. Cancer* **1997**, *75*, 202-207, doi:10.1038/bjc.1997.34.
185. Bellnier, D.A.; Gollnick, S.O.; Camacho, S.H.; Greco, W.R.; Cheney, R.T. Treatment with the tumor necrosis factor-alpha-inducing drug 5,6-dimethylxanthenone-4-acetic acid enhances the antitumor activity of the photodynamic therapy of RIF-1 mouse tumors. *Cancer Res.* **2003**, *63*, 7584-7590.
186. Krosl, G.; Korbelik, M.; Krosl, J.; Dougherty, G.J. Potentiation of photodynamic therapy-elicited antitumor response by localized treatment with granulocyte-macrophage colony-stimulating factor. *Cancer Res.* **1996**, *56*, 3281-3286.
187. Mauro, N.; Utzeri, M.A.; Varvara, P.; Cavallaro, G. Functionalization of Metal and Carbon Nanoparticles with Potential in Cancer Theranostics. *Molecules* **2021**, *26*, 3085, doi:10.3390/molecules26113085.

188. Goldberg, M.S.; Hook, S.S.; Wang, A.Z.; Bulte, J.W.; Patri, A.K.; Uckun, F.M.; Cryns, V.L.; Hanes, J.; Akin, D.; Hall, J.B.; et al. Biotargeted nanomedicines for cancer: Six tenets before you begin. *Nanomedicine* **2013**, *8*, 299-308, doi:10.2217/nnm.13.3.
189. Pellico, J.; Ellis, C.M.; Davis, J.J. Nanoparticle-Based Paramagnetic Contrast Agents for Magnetic Resonance Imaging. *Contrast Media Mol. Imaging* **2019**, 1845637, doi:10.1155/2019/1845637.
190. Lee, D.; Kwon, S.; Jang, S.Y.; Park, E.; Lee, Y.; Koo, H. Overcoming the obstacles of current photodynamic therapy in tumors using nanoparticles. *Bioact. Mater.* **2022**, *8*, 20-34, doi:10.1016/j.bioactmat.2021.06.019.
191. Vauthier, C.; Bouchemal, K. Methods for the preparation and manufacture of polymeric nanoparticles. *Pharm. Res.* **2009**, *26*, 1025-1058, doi:10.1007/s11095-008-9800-3.
192. Hoshyar, N.; Gray, S.; Han, H.; Bao, G. The effect of nanoparticle size on in vivo pharmacokinetics and cellular interaction. *Nanomedicine* **2016**, *11*, 673-692, doi:10.2217/nnm.16.5.
193. Guan, Q.; Zhou, L.L.; Li, Y.A.; Dong, Y.B. A nanoscale metal-organic framework for combined photodynamic and starvation therapy in treating breast tumors. *Chem. Commun.* **2019**, *55*, 14898-14901, doi:10.1039/c9cc07510k.
194. Wan, S.S.; Zeng, J.Y.; Cheng, H.; Zhang, X.Z. ROS-induced NO generation for gas therapy and sensitizing photodynamic therapy of tumor. *Biomaterials* **2018**, *185*, 51-62, doi:10.1016/j.biomaterials.2018.09.004.
195. Miyoshi, N.; Kundu, S.K.; Tuziuti, T.; Yasui, K.; Shimada, I.; Ito, Y. Combination of Sonodynamic and Photodynamic Therapy against Cancer Would Be Effective through Using a Regulated Size of Nanoparticles. *Nanosci. Nanoeng.* **2016**, *4*, 1-11, doi:10.13189/nn.2016.040101.
196. Liu, D.L.; Andersson-Engels, S.; Sturesson, C.; Svanberg, K.; Hakansson, C.H.; Svanberg, S. Tumour vessel damage resulting from laser-induced hyperthermia alone and in combination with photodynamic therapy. *Cancer Lett.* **1997**, *111*, 157-165, doi:10.1016/s0304-3835(96)04528-4.